SAND2015-8397C

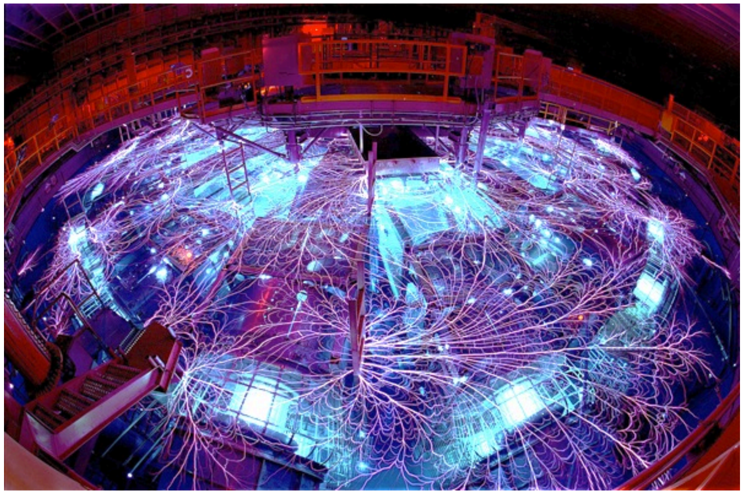

Sandia National Laboratories

Exceptional service in the national interest

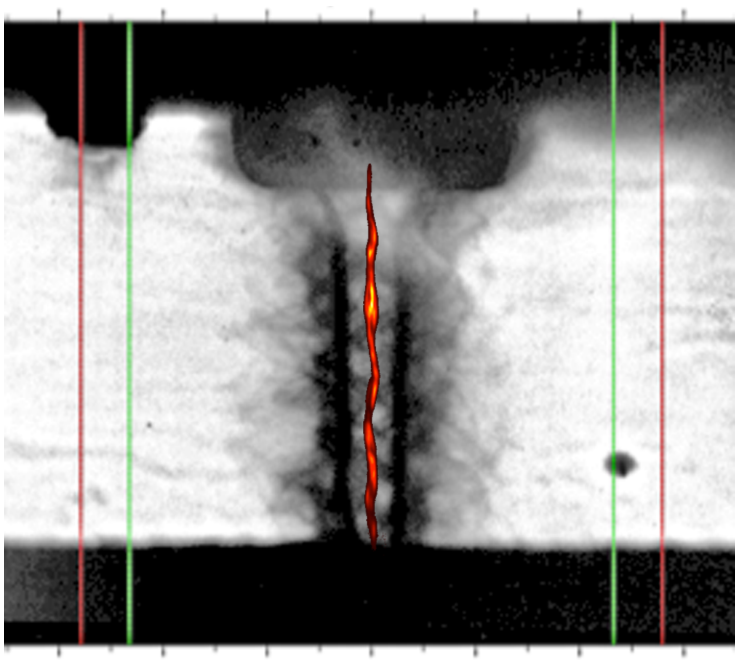

Comparison between simulations and initial MagLIF experiments

A. B. Sefkow for the MagLIF team
Sandia National Laboratories, Albuquerque, NM

International Conference on
Inertial Fusion Sciences and Applications

Seattle, Washington, USA
September 22nd, 2015

SAND2015-5089 C

Collaborators

Sandia National Laboratories

J. M. Koning[2], T. J. Awe[1], B. E. Blue[3], E. L. M. Campbell[1], G. A. Chandler[1], K. Cochrane[1], M. E. Cuneo[1], M. Geissel[1], M. R. Gomez[1], K. D. Hahn[1], S. B. Hansen[1], E. C. Harding[1], A. J. Harvey-Thompson[1], M. H. Hess[1], C. Jennings[1], M. W. Kimmel[1], P. F. Knapp[1], D. C. Lamppa[1], J. Lash[1], B. G. Logan[2], M. M. Marinak[2], R. D. McBride[1], K. J. Peterson[1], J. L. Porter[1], P. K. Rambo[1], G. A. Rochau[1], D. V. Rose[4], D. Rovang[1], C. L. Ruiz[1], P. F. Schmit[1], M. Schollmeier[1], D. G. Schroen[3], J. Schwarz[1], D. B. Sinars[1], S. A. Slutz[1], I.C. Smith[1], W. Stygar[1], C. Thoma[4], K. Tomlinson[3], R. A. Vesey[1], D. R. Welch[4], and their associated teams

[1] Sandia National Laboratories, Albuquerque, NM
[2] Lawrence Livermore National Laboratory, Livermore, CA
[3] General Atomics, San Diego, CA
[4] Voss Scientific, Albquerque, NM

Many groups want to use magnetic fields to relax inertial fusion stagnation requirements

SNL Phi Target

1982 Demonstration of enhanced fusion yield with magnetization (~1e6 DD yield)

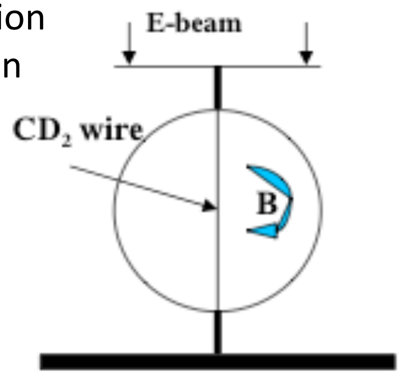

Max Planck/ITEP

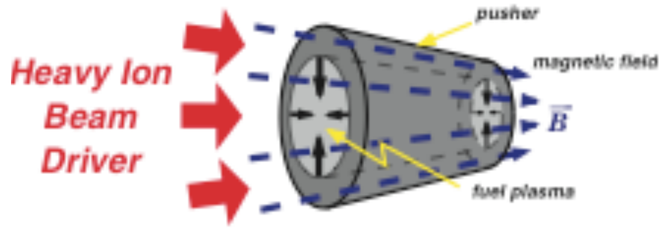

Basko, Kemp, Meyer-ter-Vehn, *Nucl. Fusion* **40**, 59 (2000)
Kemp, Basko, Meyer-ter-Vehn, *Nucl. Fusion* **43**, 16 (2003)

LLNL

(Perkins *et al.*, Phys Plasmas 2013)

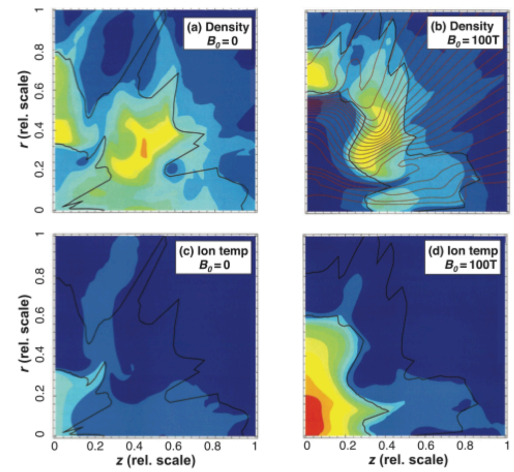

University of Rochester/LLE

2011 Demonstration of enhanced fusion yield with magnetization (~5e9 DD yield)

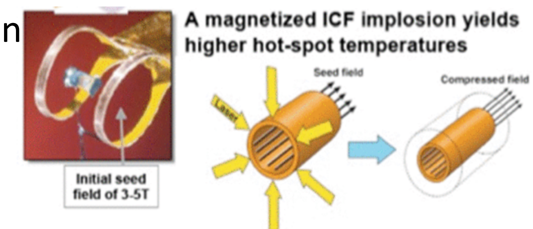

Gotchev *et al.*, *Rev. Sci. Instr.* **80**, 043504 (2009)

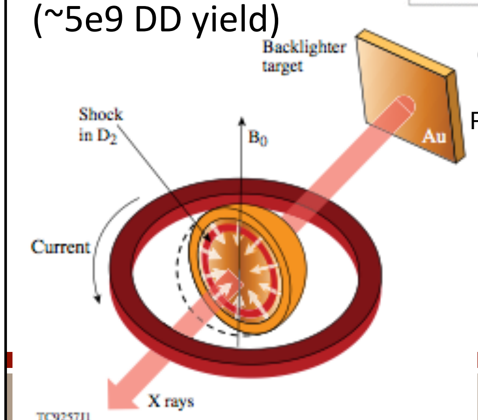

P.Y. Chang *et al.*, PRL (2011).

Los Alamos/Air Force Research Lab

Field Reversed Configuration FRC
Magnetic Target Fusion
Shiva Star
closed field lines
FRC

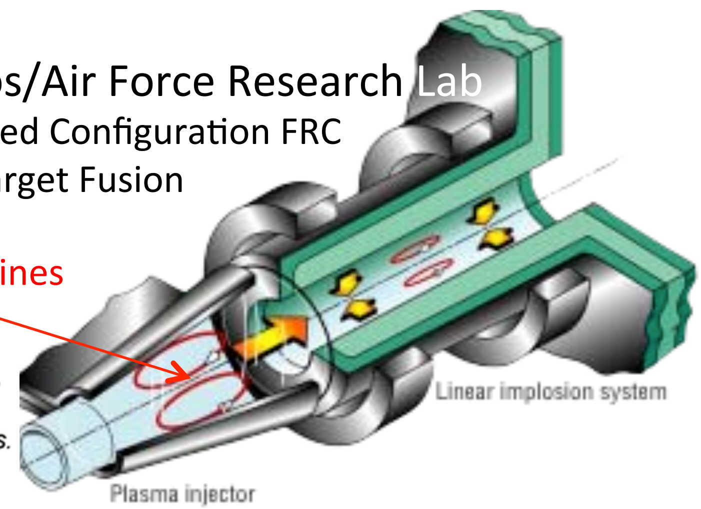

Taccetti, Intrator, Wurden *et al.*, *Rev. Sci, Instr.* **74**, 4314 (2003)
Degnan *et al.*, *IEEE Trans. Plas. Sci.* **36**, 80 (2008)

and many others…

"Z" is the world's largest pulsed-power facility

Sandia National Laboratories

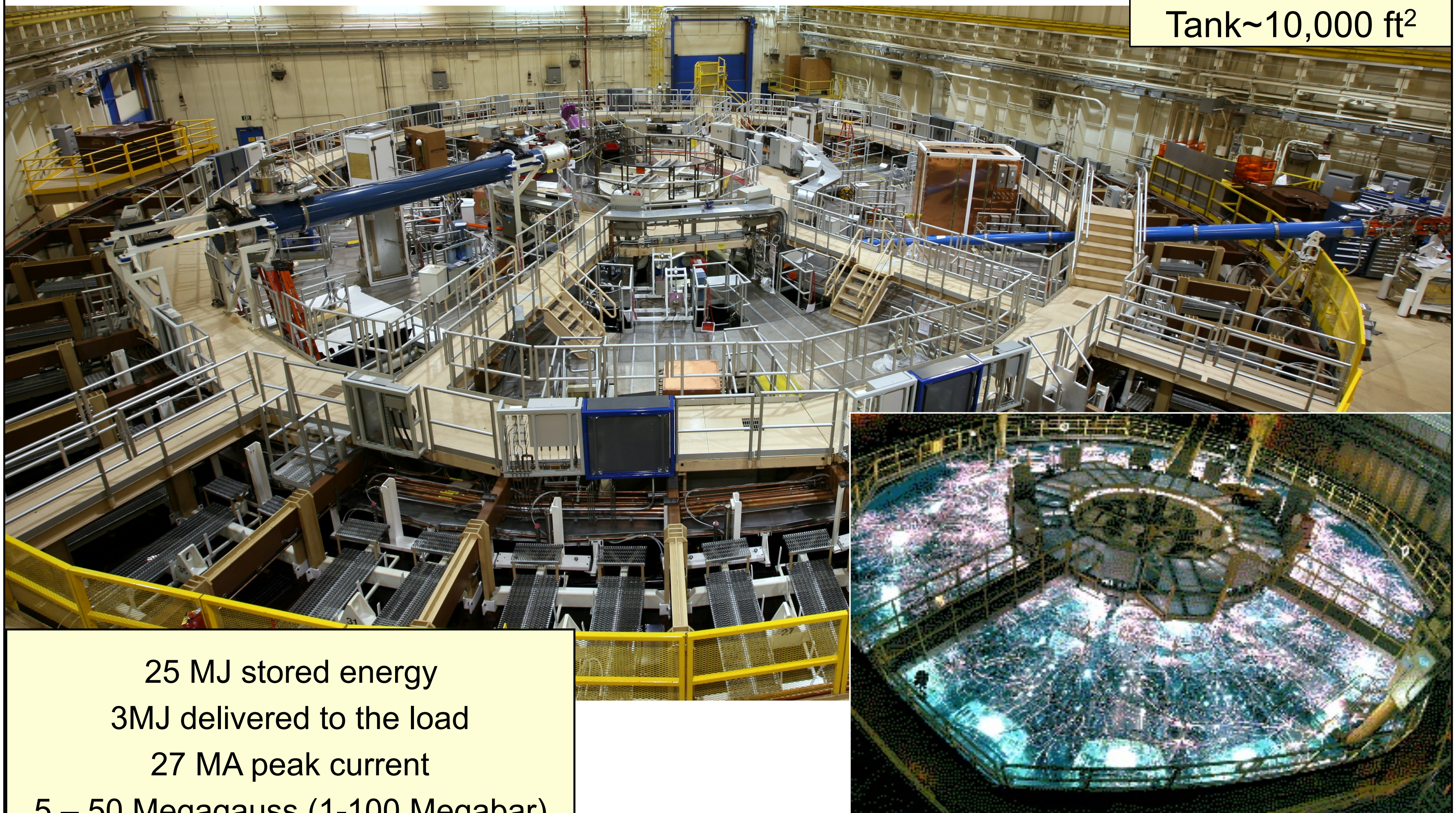

Tank~10,000 ft^2

25 MJ stored energy
3MJ delivered to the load
27 MA peak current
5 – 50 Megagauss (1-100 Megabar)
100-600 ns pulse length

We are working toward the evaluation of the Magnetized Liner Inertial Fusion concept

- An **initial B_z~10-40 T** flux is compressed to ~5-15 kT (~50-150 MG)
  - to reduce thermal electron conduction losses
  - to enable low ρR_{fuel} ignition ($B_z R_{fuel}$ and ρR_{liner} required instead)
- The fuel is **preheated** using the Z-Beamlet laser in order to reduce:
  - the convergence ratio (CR) needed to obtain T_{ion} > 4 keV
  - the implosion velocity needed to ≤ 100 km/s
  - the stagnation pressure needed to a few Gbar (not 100s Gbar)
- ***Thermonuclear yields have been measured on Z***

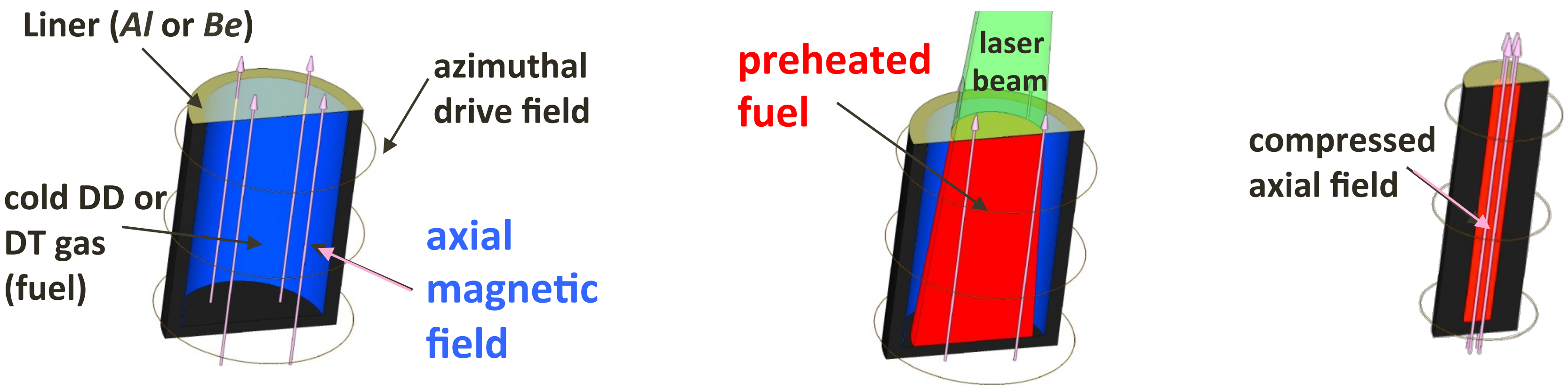

S. A. Slutz, et. al., Phys. Plasmas 17, 056303 (2010).

Z is used to compress a liner containing pre-magnetized and pre-heated D_2 gas

Sandia National Laboratories

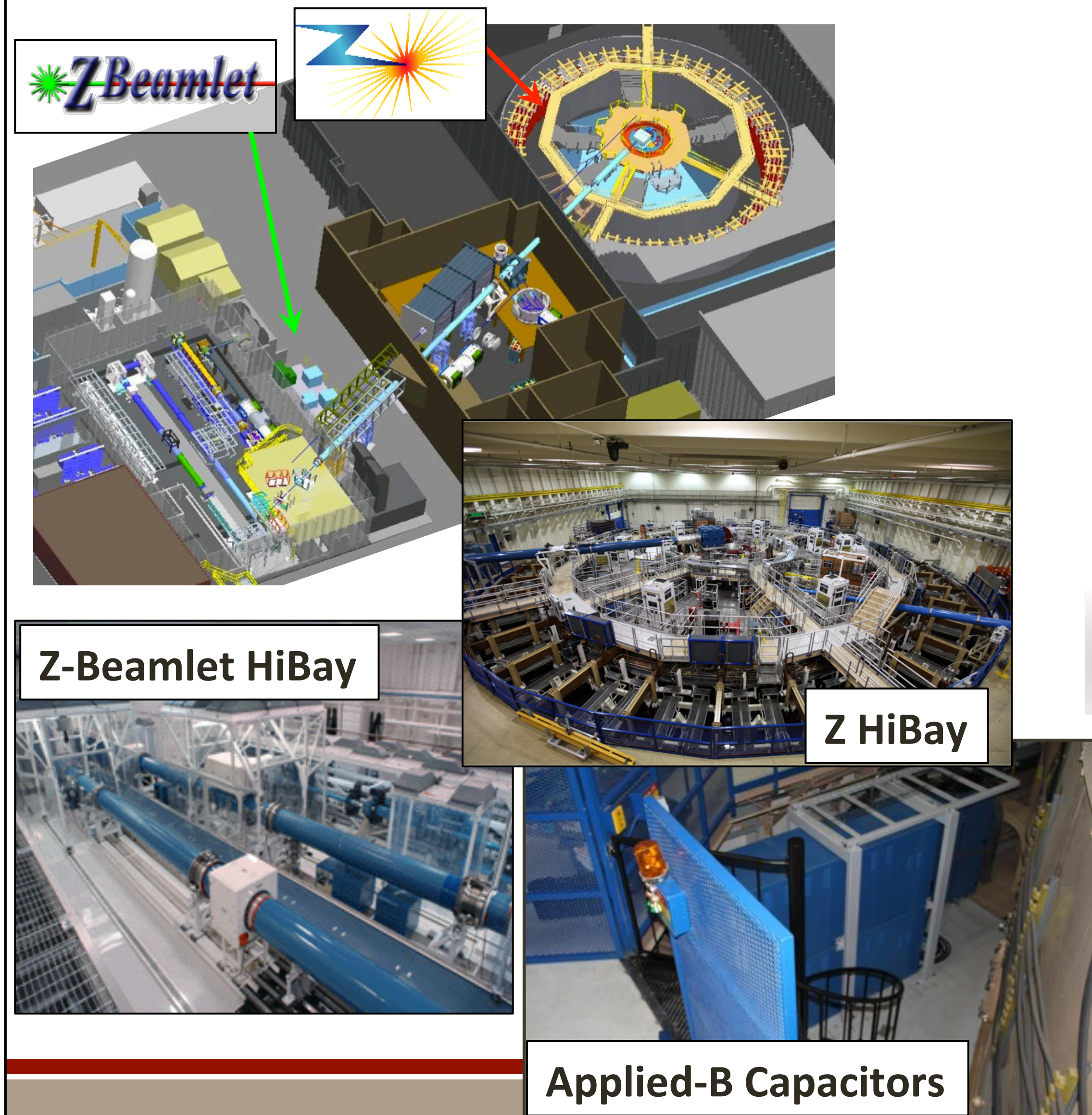

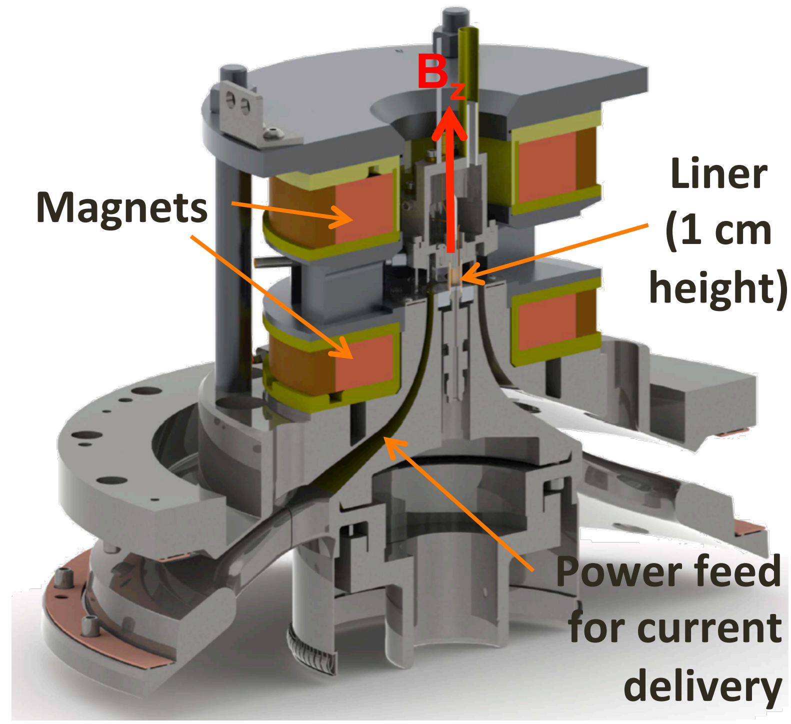

SAND2015-5089 C

The first fully-integrated MagLIF experiments successfully demonstrated the concept

Sandia National Laboratories

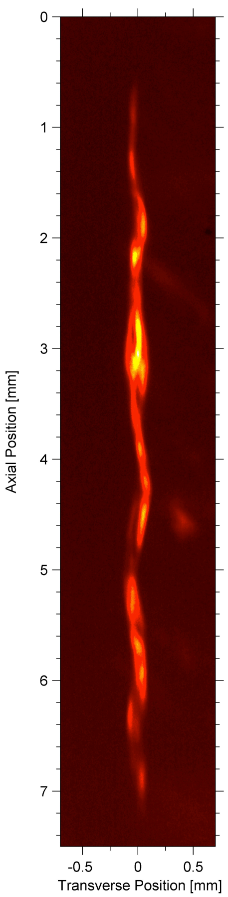

- Thermonuclear neutron generation up to 2e12
- Fusion-relevant stagnation temperatures
- Stable pinch with narrow emission column at stagnation
- Successful flux compression

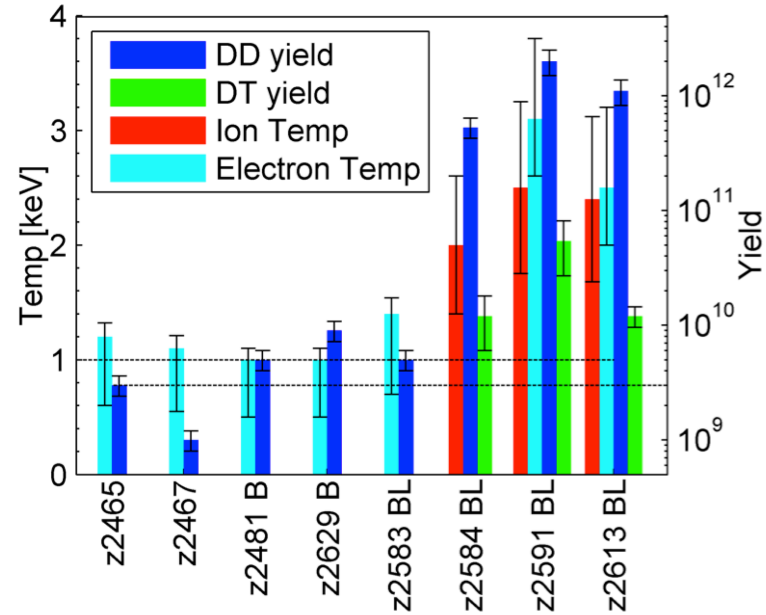

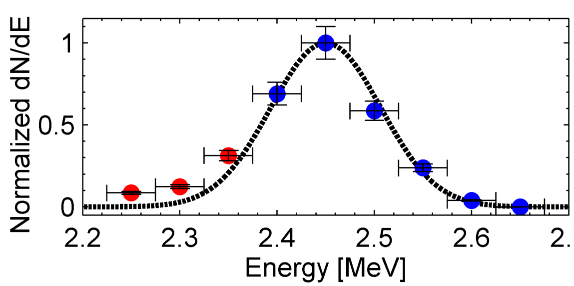

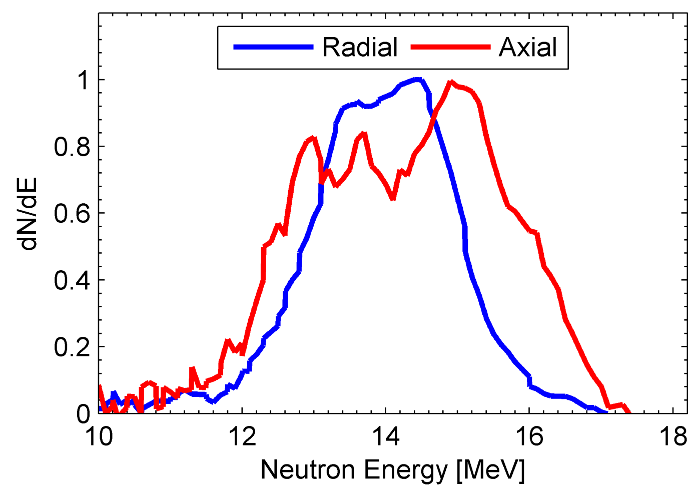

An **integrated** model seeks to realistically simulate experiments as they would occur on Z

Sandia National Laboratories

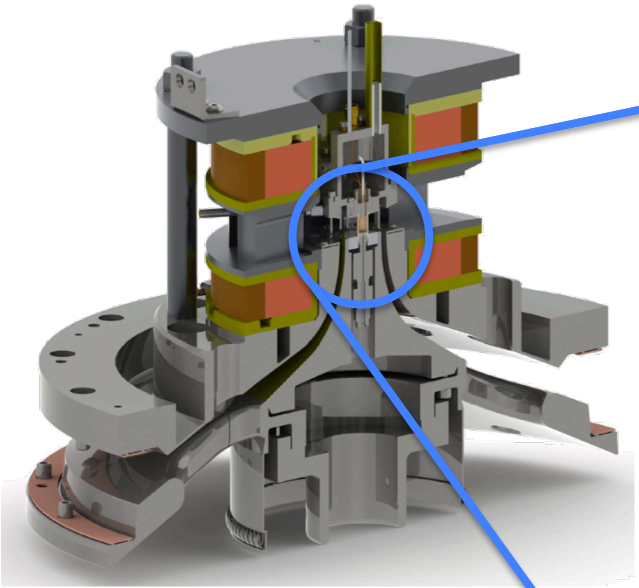

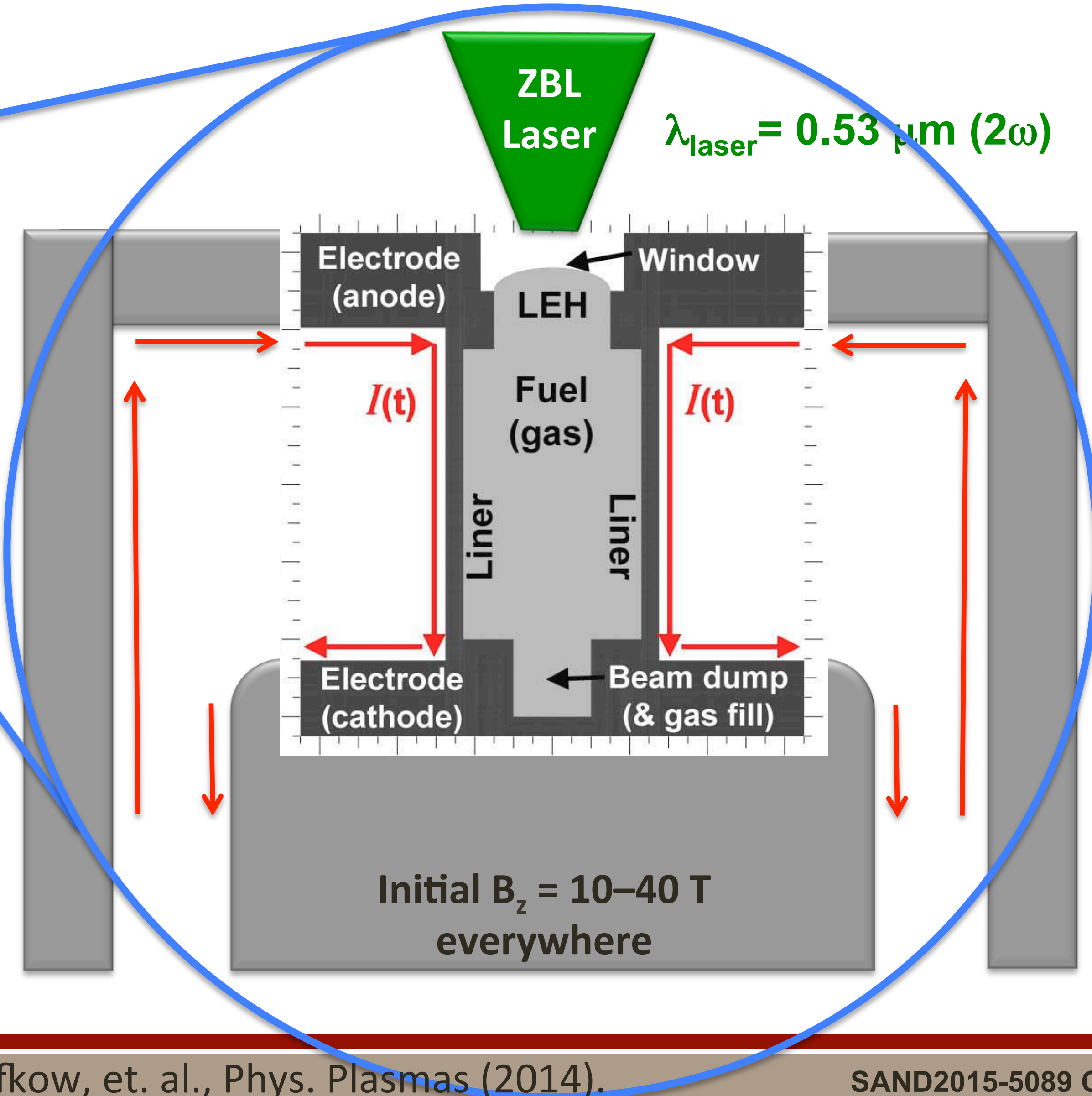

Self-consistently integrated into one simulation:

(1) Laser
(2) Laser entrance hole (LEH) and window
(3) Liner and circuit
(4) Electrode end caps
(5) Component interactions, timing, and optimization

A. B. Sefkow, et. al., Phys. Plasmas (2014).

An integrated model seeks to realistically simulate experiments as they would occur on Z

And 3D is required for helical (B_θ+B_z) magneto-RT growth and any 3D laser effects

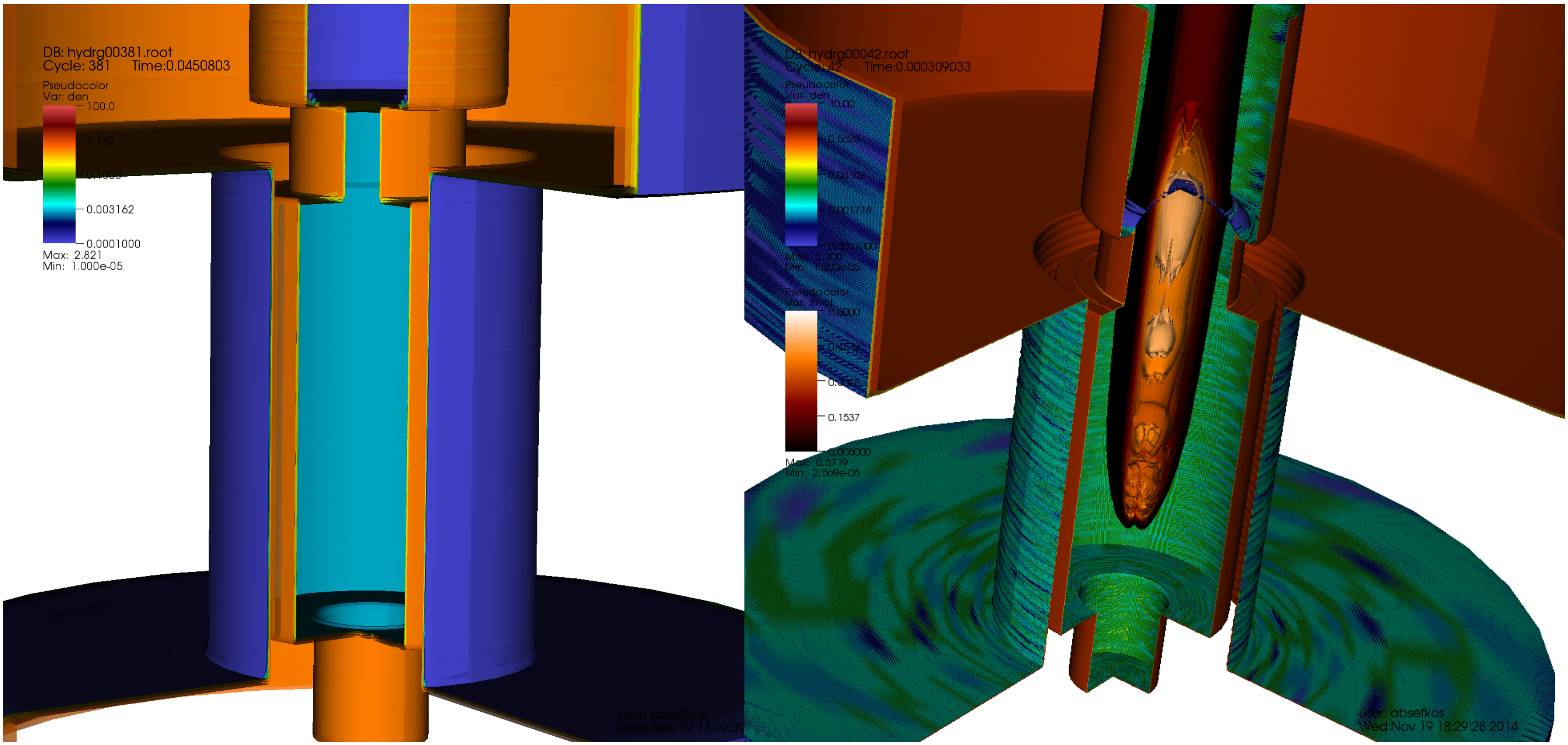

Laser-energy coupling reduction for near-term integrated experiments on Z

If the energy absorbed by the gas is less than the optimal amount (due to low window transmission and/or LPI), temperature and yield reductions would be expected.

The effect is approximated with a series of integrated calculations wherein the main pulse energy is decreased from full to none.

The experimental yields may be consistent with low transmitted laser energies measured in related “focused” experiments

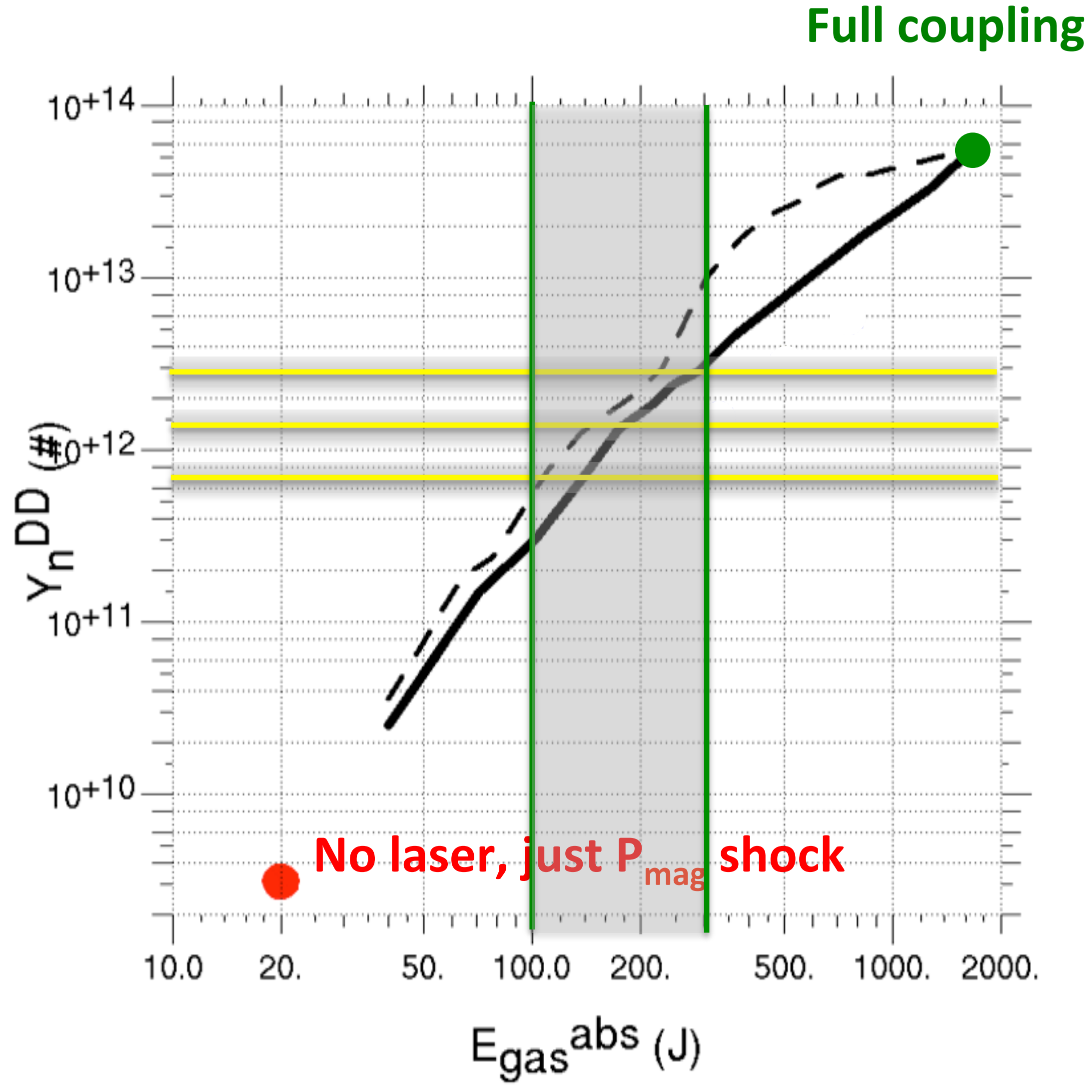

A. B. Sefkow, et. al., Phys. Plasmas (2014).

Estimate for laser depositions through a 3.4 μm window transmission is ~200 J

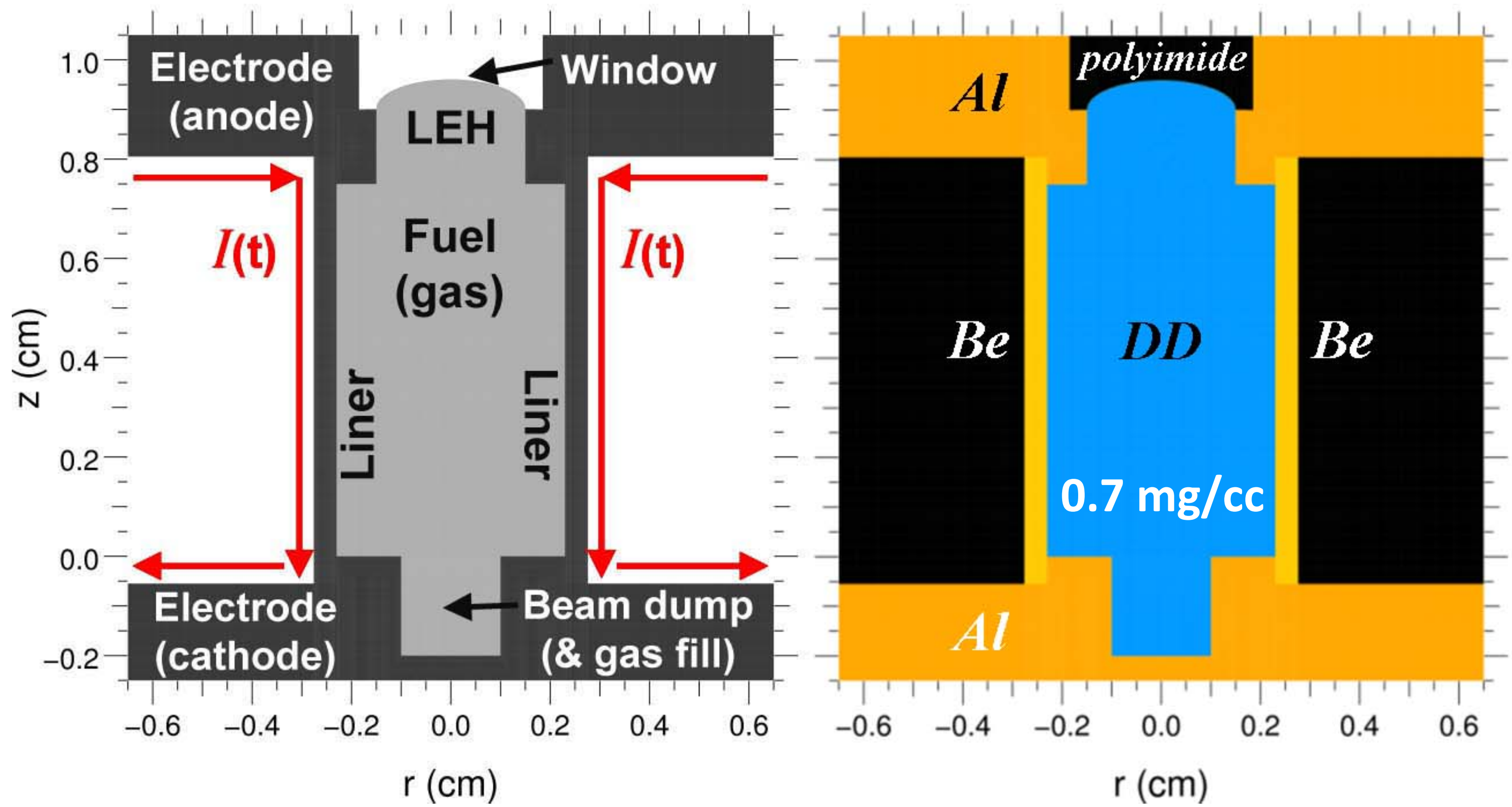

Estimate for laser depositions through a 3.4 μm window transmission is ~200 J

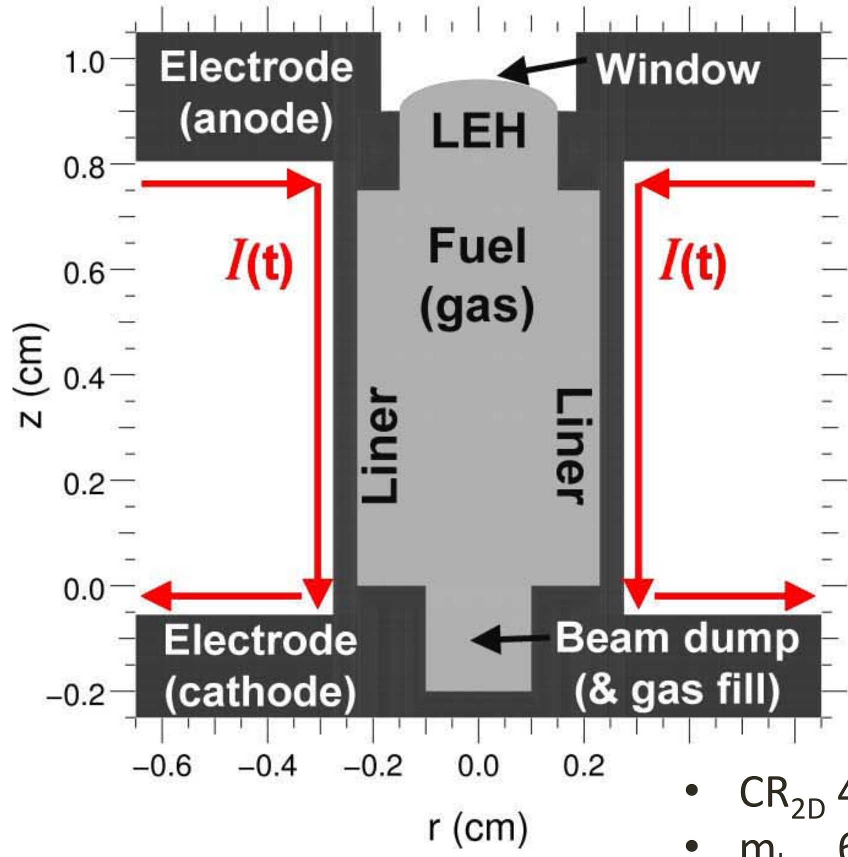

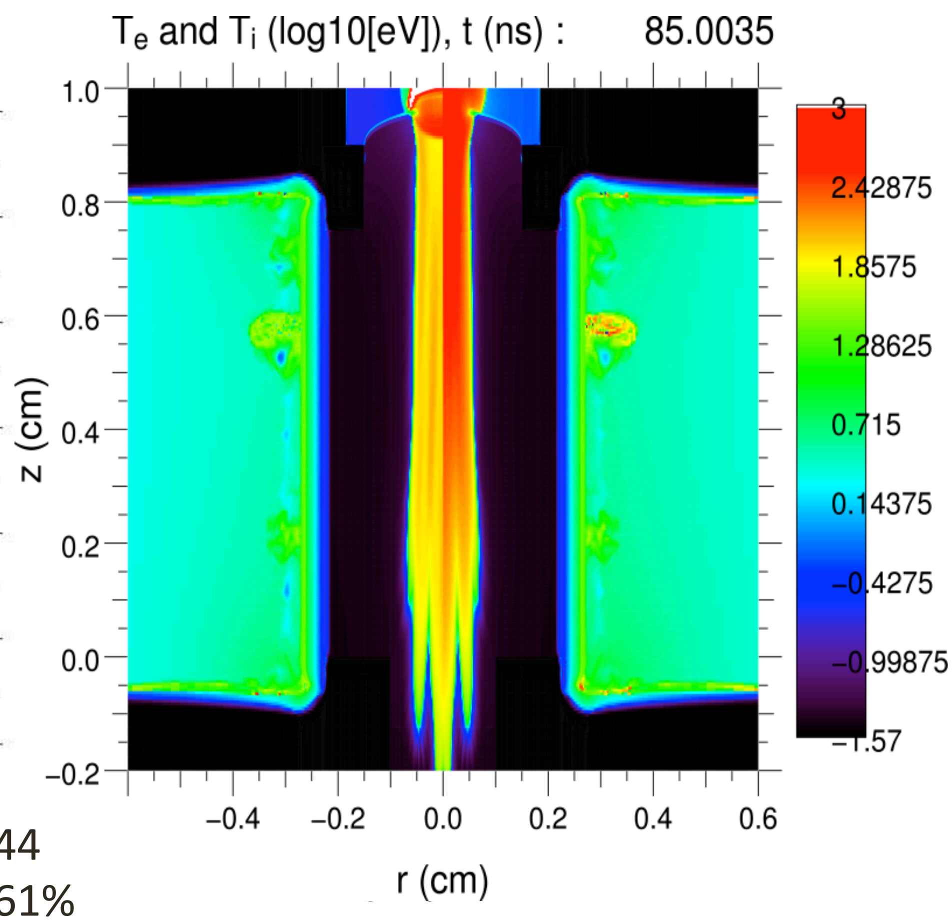

- CR_{2D} 44
- m_{loss} 61%
- Φ_{loss} 53%
- $\langle T_i \rangle^{DD}$ 3.0 keV
- $\langle T_{e/i} \rangle$ 2.7 keV

Current and implosion time agree within error

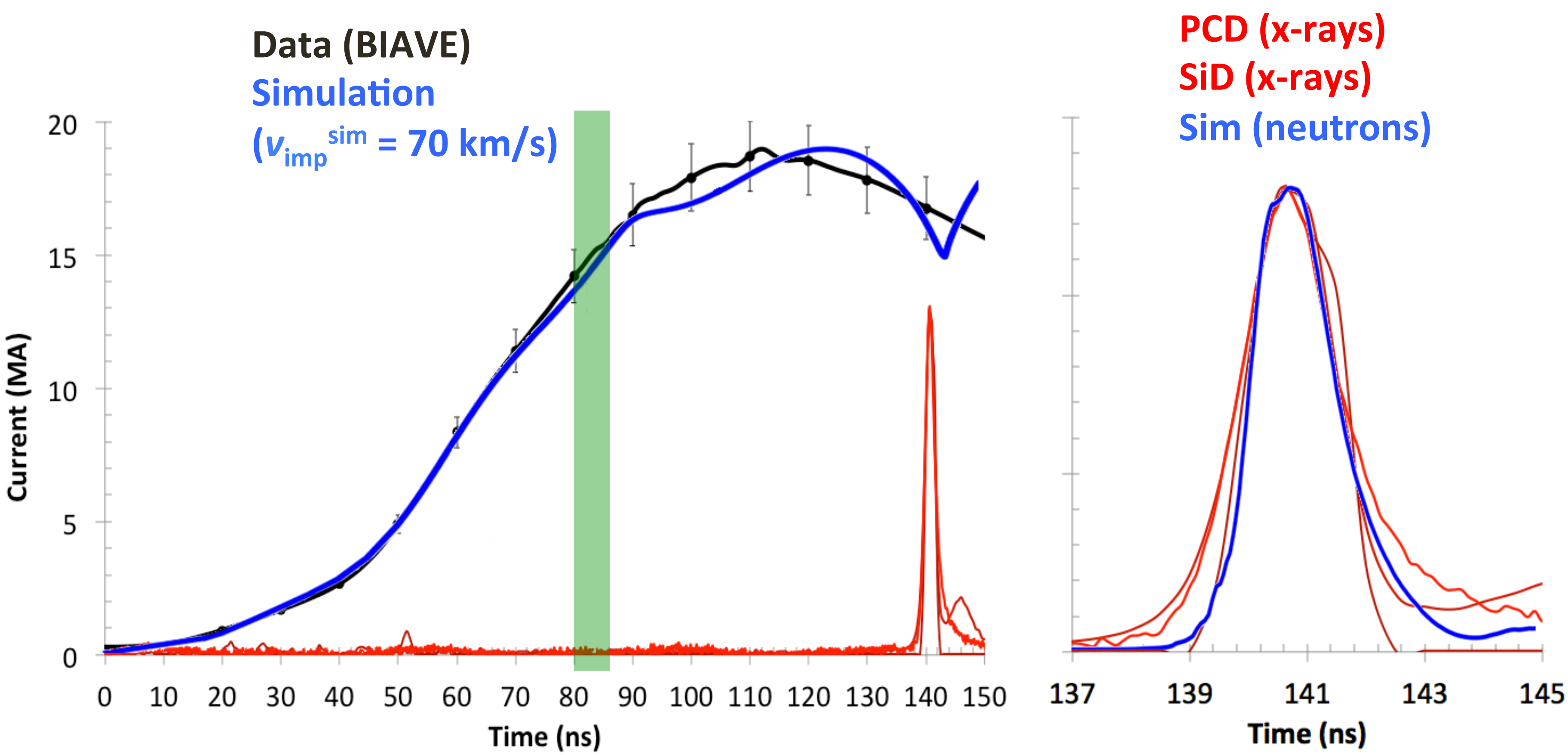

Radiographs of magnetized liners were helically perturbed and suggested enhanced stability

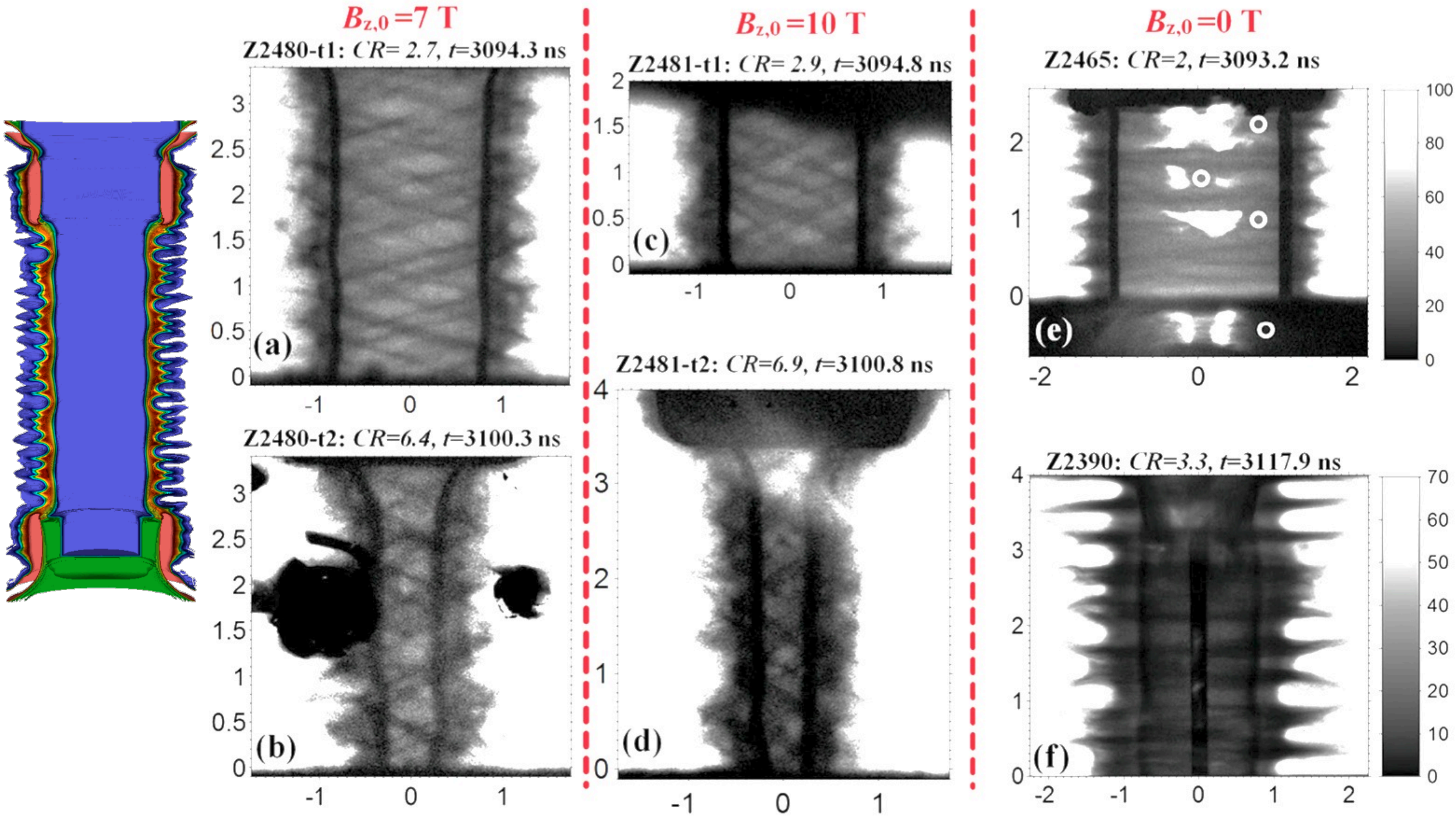

T. J. Awe., et. al., *Phys. Rev. Lett.* (2013)

SAND2015-5089 C

Comparison of stagnation column shape, not accounting for liner instability or opacity

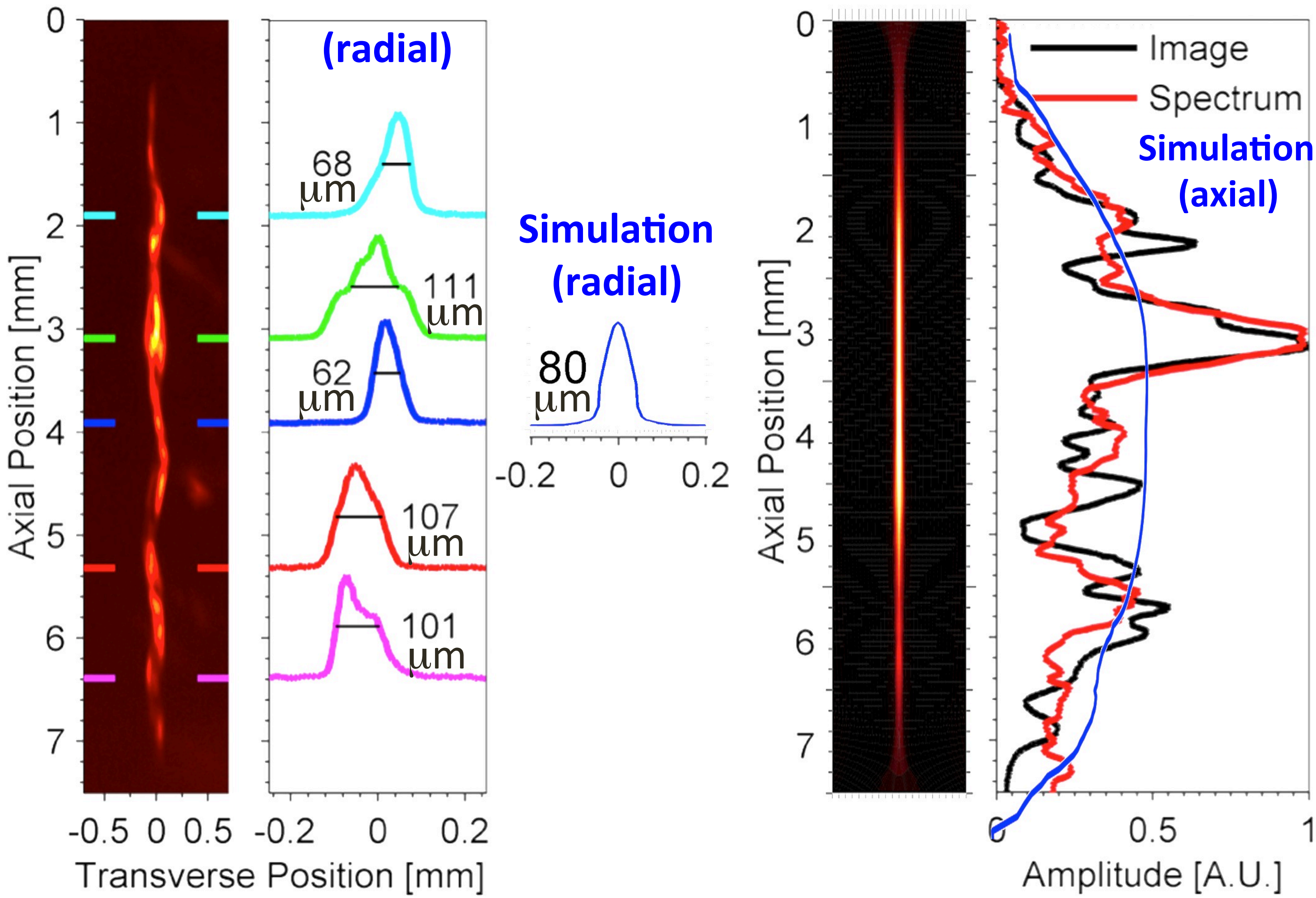

Variation in self-emission and liner opacity contribute to observed structure

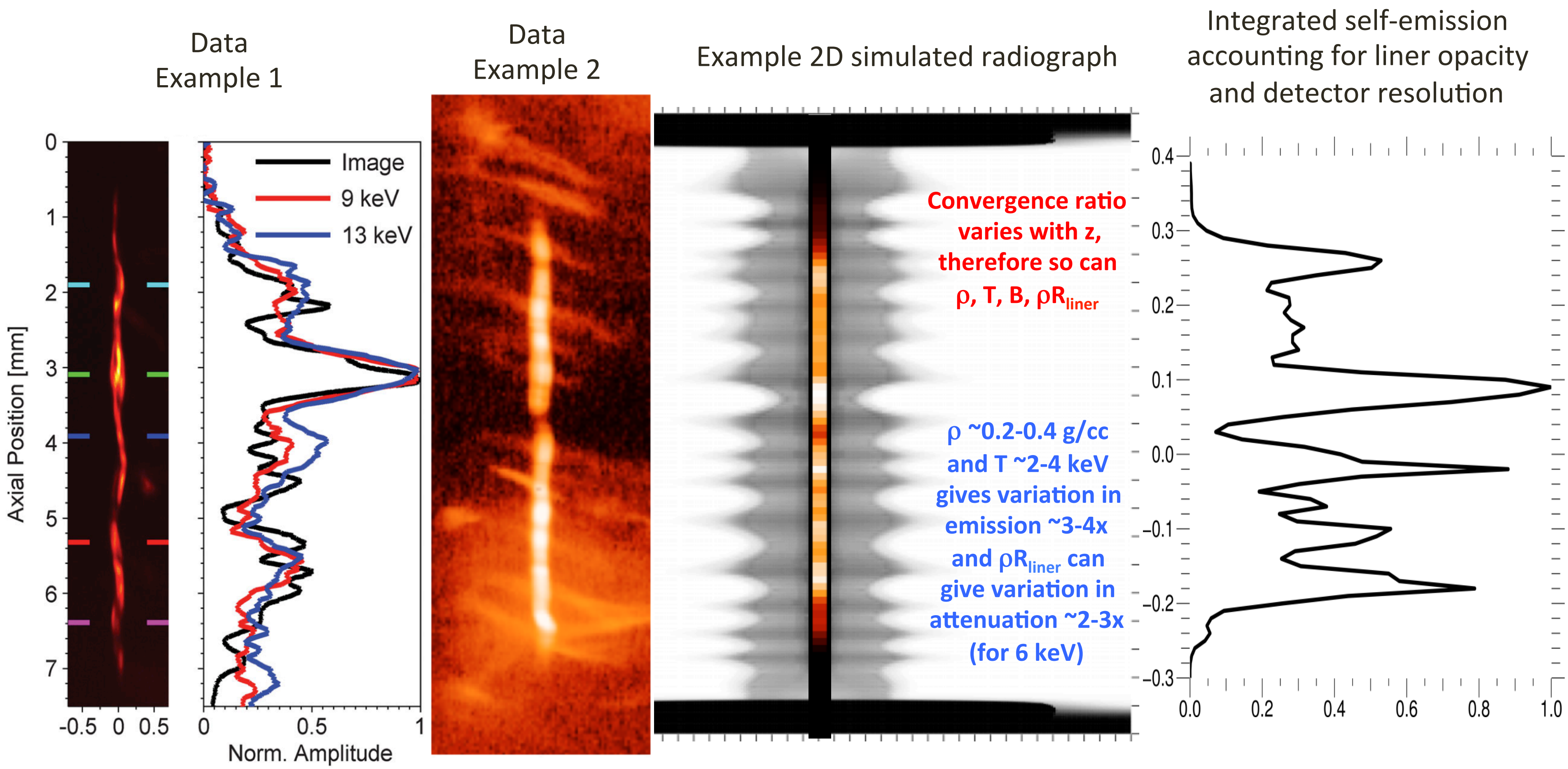

However, helical emission and radiographs require 3D simulations

In 3D with B_z, simulations show helical perturbations grow as well as improve stability due to m=0 suppression

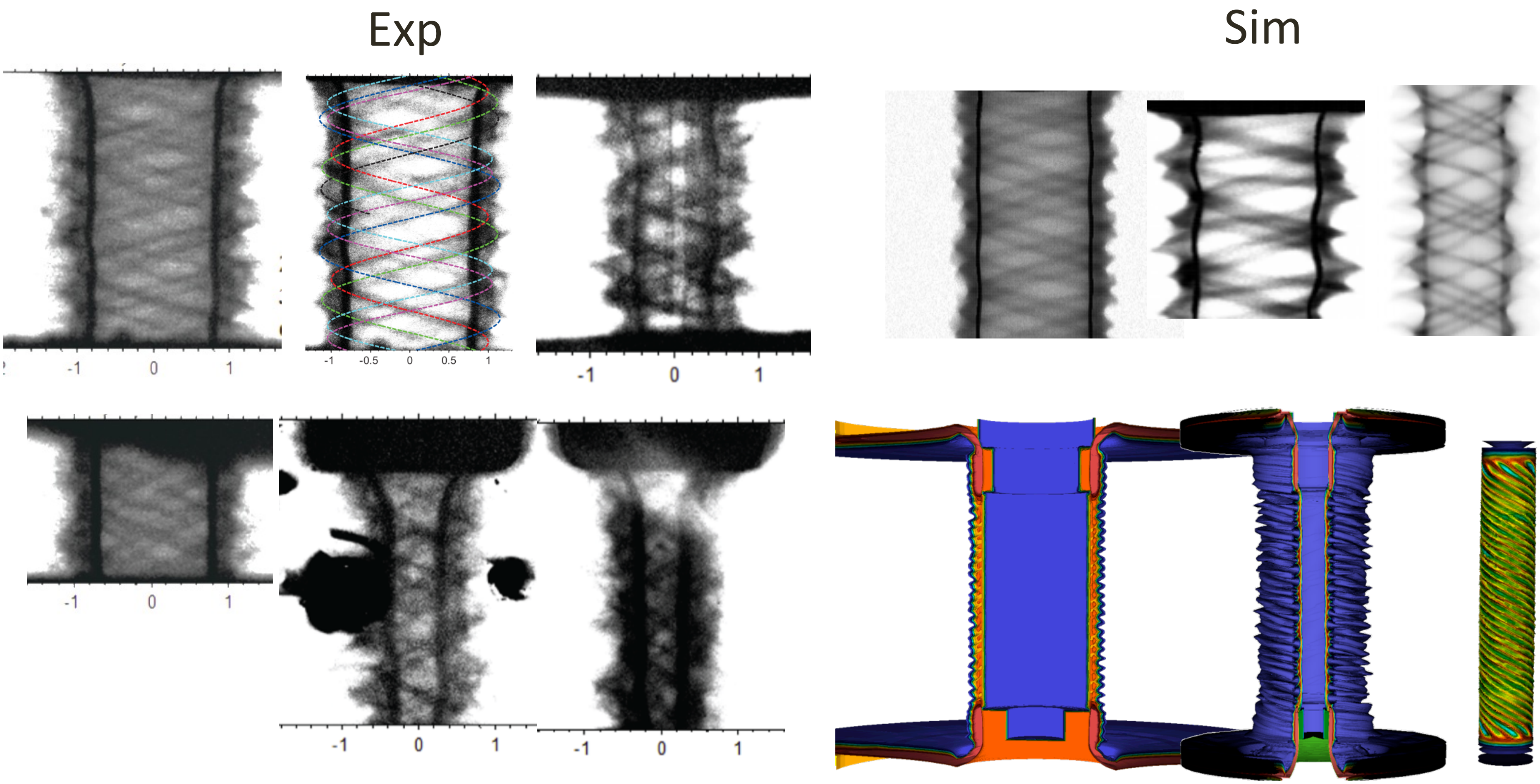

Imposed helical perturbation grows w/ constant pitch and enables high convergence ratio implosions

Full 3D with helical instability growth is needed to correctly simulate the stagnation column

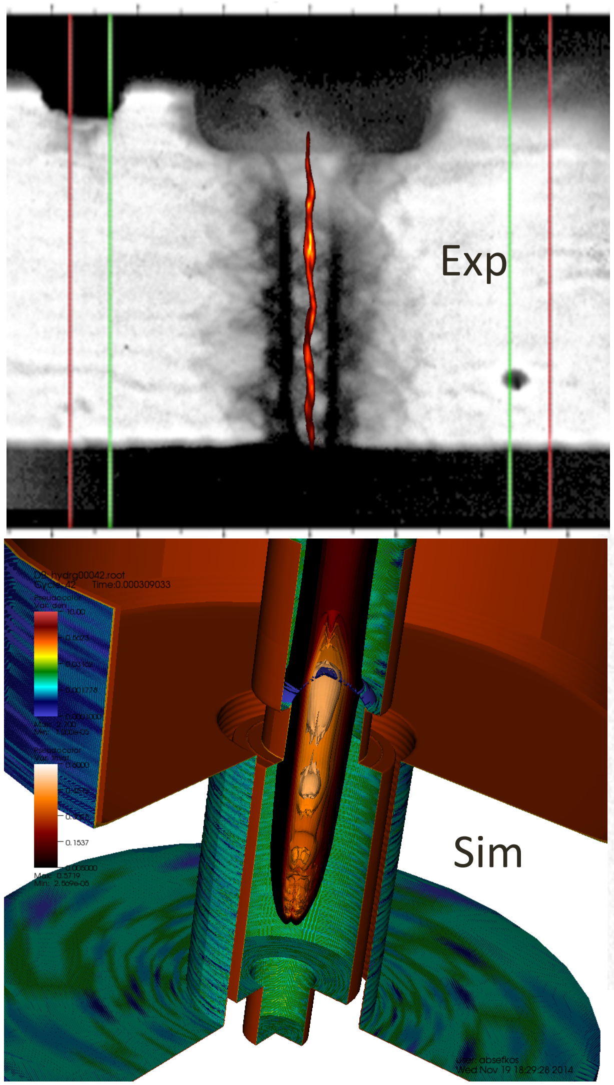

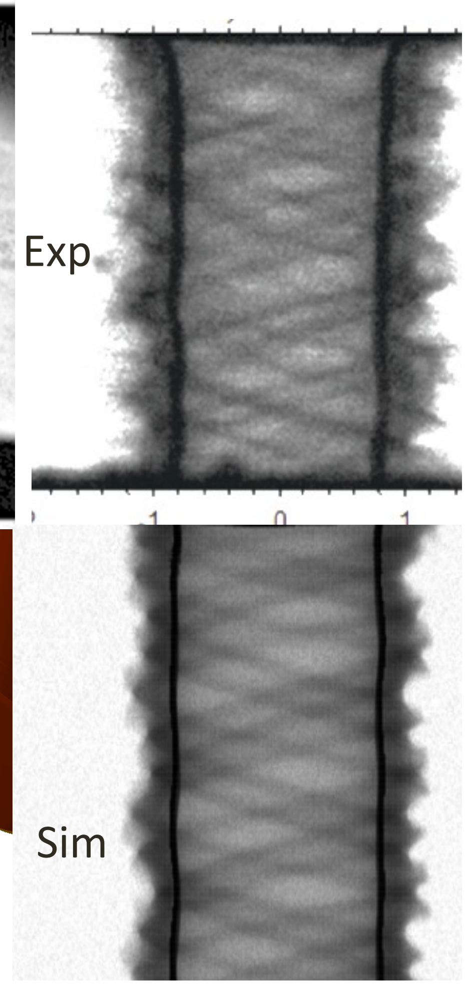

From fluid simulation using perturbation from kinetic simulation

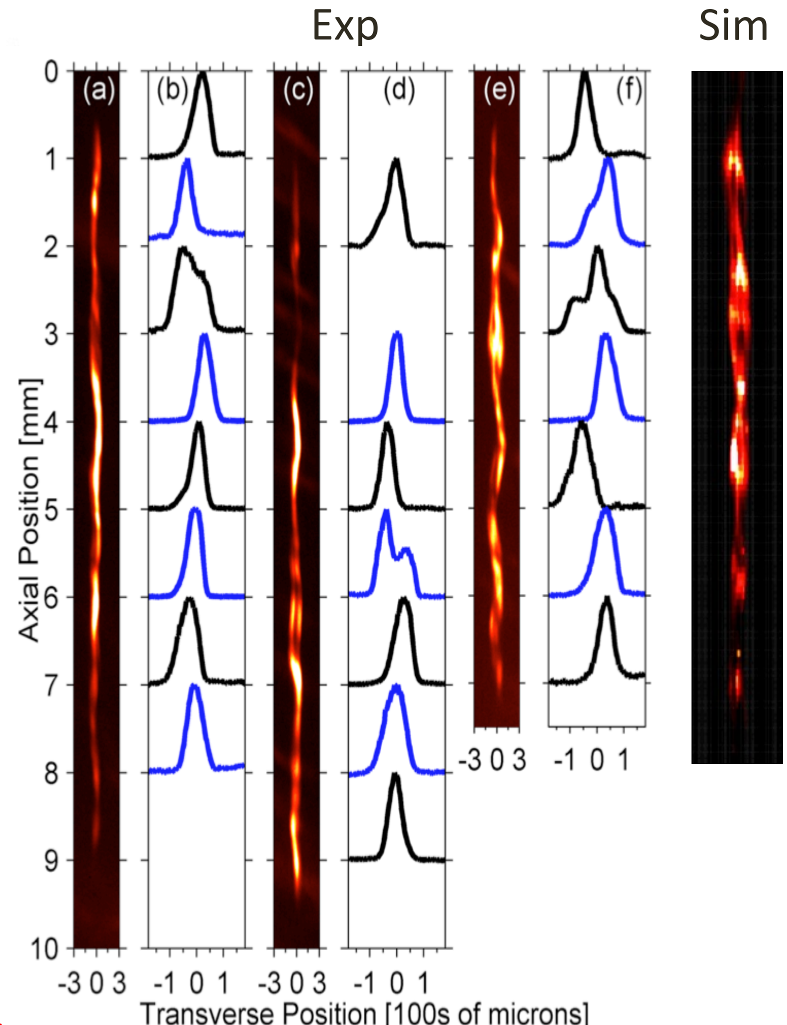

Trend of helical perturbation with imposed B_z as predicted by first principles PIC simulation

Sandia National Laboratories

B_z = + 10 T | B_z = + 7 T | B_z = 0 T | B_z = - 10 T

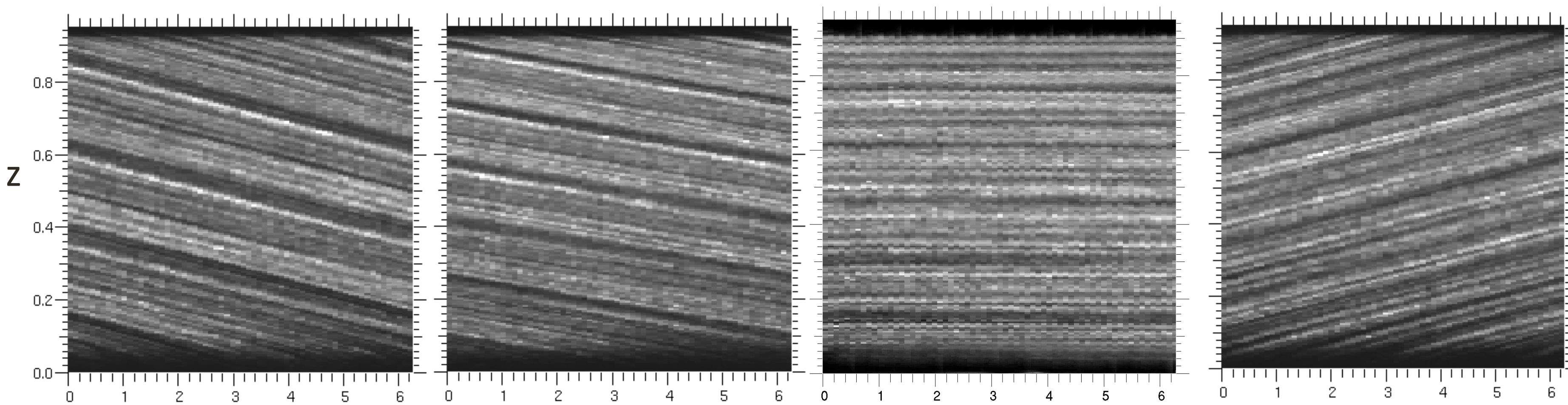

ϕ ~ 7.5-8.2° | ϕ ~ 5.2-5.8° | ϕ ~ 0° | ϕ ~ -7.5 -8.2°

B_z up | *No B_z* | *B_z down*

XUV emission on COBRA,
L. Atoyan et. al. (Cornell)
APS-DPP 2014 Poster →

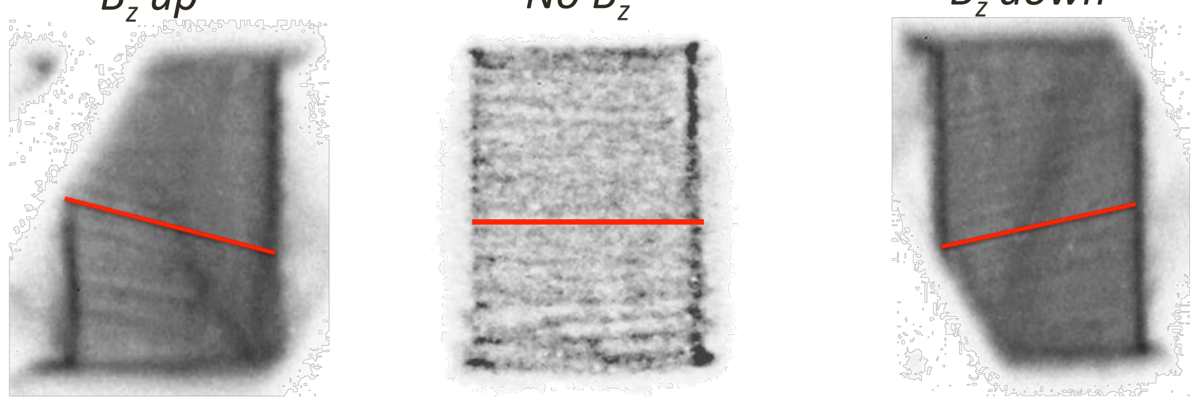

The ~0.2 and ~1.0 mm modes have implications

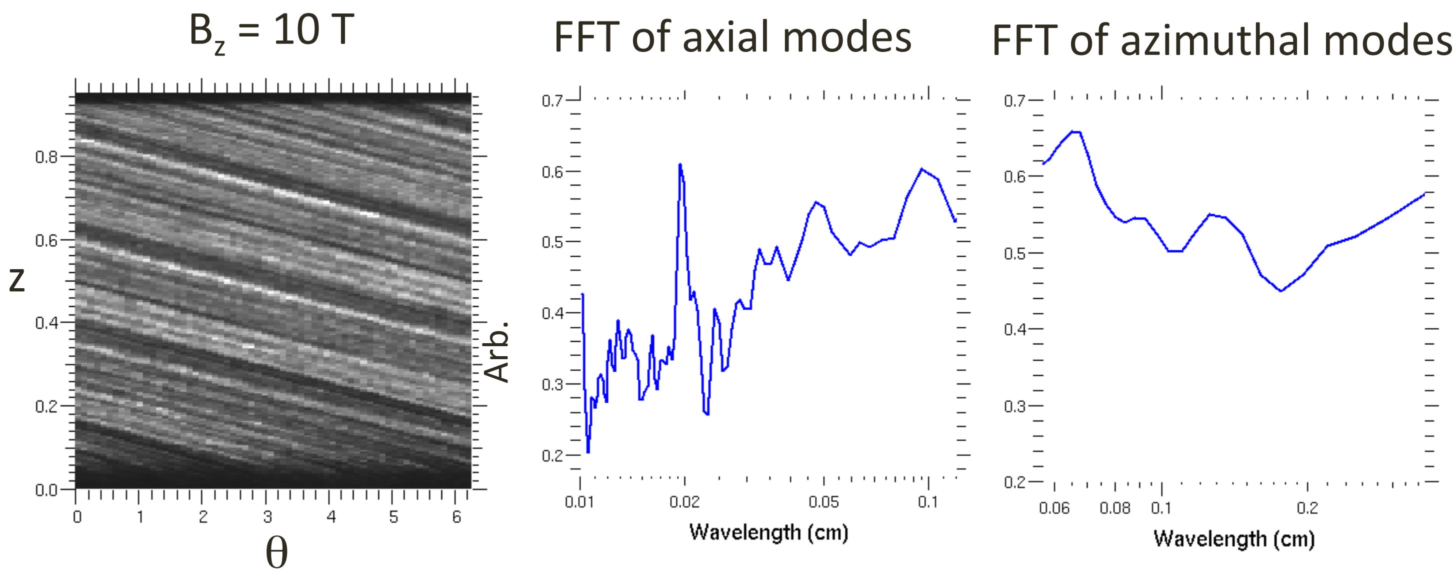

- Short axial λ_z ~0.2 mm mode gives the helical straitions in radiographs
- Long axial λ_z ~1 mm mode imprints at the liner/gas interface and gives the helical self-emission image at stagnation

Perturbation depends on load configuration, V/I, and material.

Explanation of helical stagnation mechanism

Early-time inner boundary

density

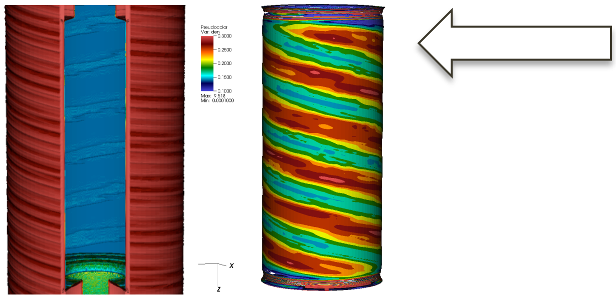

Long axial λ_z ~1 mm is from early-time feedthrough and imprints at the liner/gas interface

Explanation of helical stagnation mechanism

Early-time inner boundary *density*

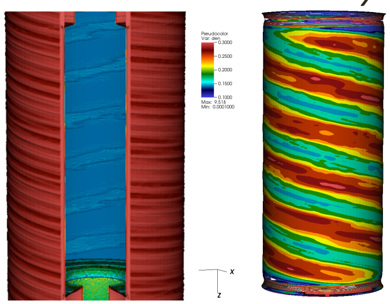

Long axial λ_z ~1 mm is from early-time feedthrough and imprints at the liner/gas interface

Since the interface is magneto-Rayleigh-Taylor stable, the gas is high β, and flux pile-up occurs there, λ_z also imprints on B_z

Inner boundary B_z

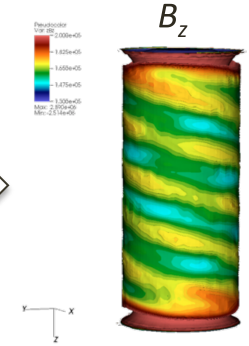

Explanation of helical stagnation mechanism

Early-time inner boundary *density*

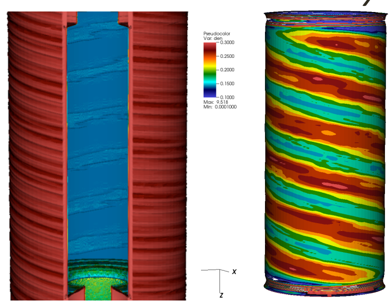

Long axial λ_z ~1 mm is from early-time feedthrough and imprints at the liner/gas interface

Since the interface is magneto-Rayleigh-Taylor stable, the gas is high β, and flux pile-up occurs there, λ_z also imprints on B_z

Inner boundary B_z

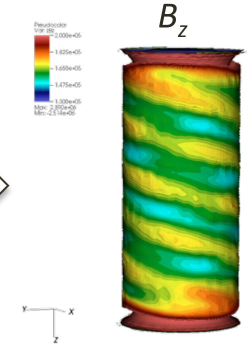

Late-time inner boundary

density B_z

z

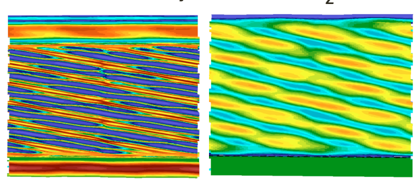

θ θ

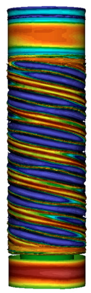

As in helical perturbation on rear side of liner, inner surface helix persists and grows as well

Explanation of helical stagnation mechanism

Early-time inner boundary

density

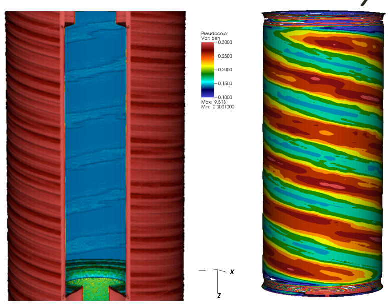

Long axial λ_z ~1 mm is from early-time feedthrough and imprints at the liner/gas interface

Since the interface is magneto-Rayleigh-Taylor stable, the gas is high β, and flux pile-up occurs there, λ_z also imprints on B_z

Inner boundary

B_z

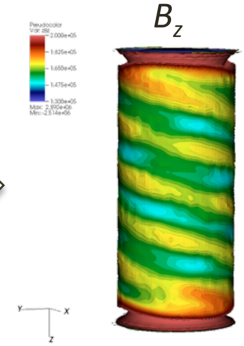

Late-time inner boundary

density B_z

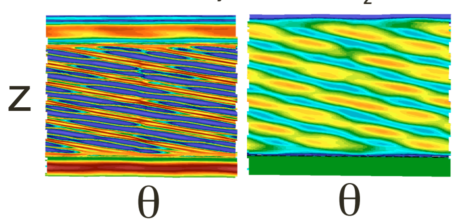

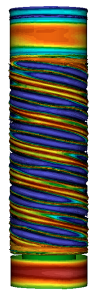

As in helical perturbation on rear side of liner, inner surface helix persists and grows as well

Resulting structure does not strongly modify 2D physics

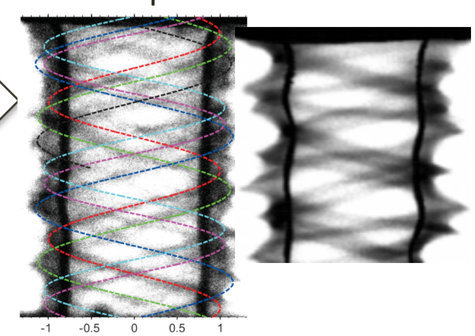

Explanation of helical stagnation mechanism

Early-time inner boundary *density*

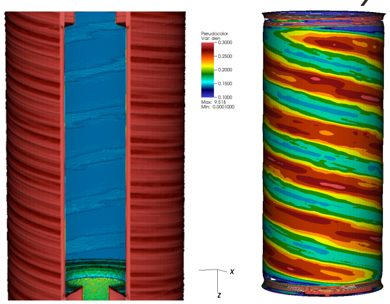

Long axial λ_z ~1 mm is from early-time feedthrough and imprints at the liner/gas interface

Inner boundary B_z

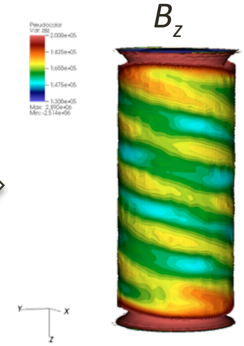

Since the interface is magneto-Rayleigh-Taylor stable, the gas is high β, and flux pile-up occurs there, λ_z also imprints on B_z

Late-time inner boundary

density B_z

z

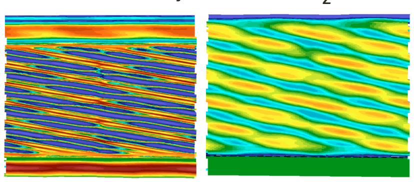

θ θ

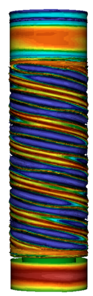

As in helical perturbation on rear side of liner, inner surface helix persists and grows as well

Exp Sim

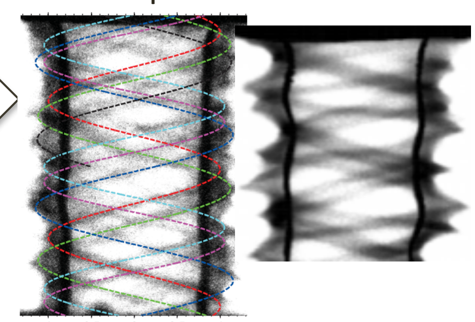

Resulting structure does not strongly modify 2D physics

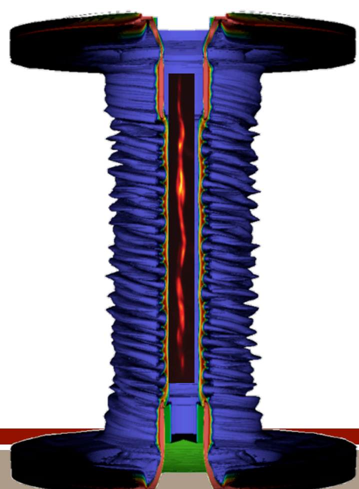

Resulting weakly helical (dr << dz) emitting stagnation column remains quasi-2D such that $P_{stag}^{exp} \sim P_{stag}^{3D} \sim P_{stag}^{2D} \sim 1$ Gbar

Explanation of helical stagnation mechanism

Early-time inner boundary *density*

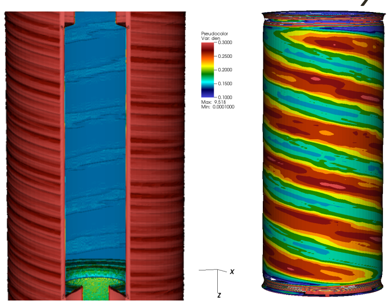

Long axial λ_z ~1 mm is from early-time feedthrough and imprints at the liner/gas interface

Inner boundary B_z

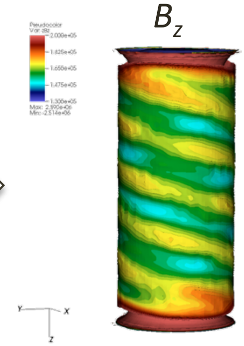

Since the interface is magneto-Rayleigh-Taylor stable, the gas is high β, and flux pile-up occurs there, λ_z also imprints on B_z

Late-time inner boundary

density B_z

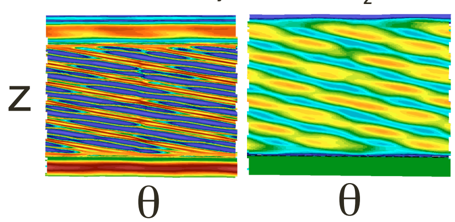

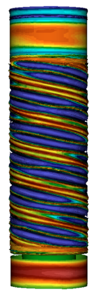

As in helical perturbation on rear side of liner, inner surface helix persists and grows as well

Exp Sim

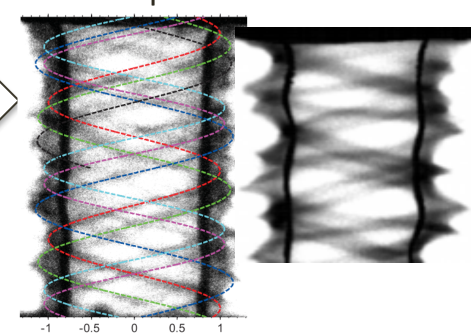

Resulting structure does not strongly modify 2D physics

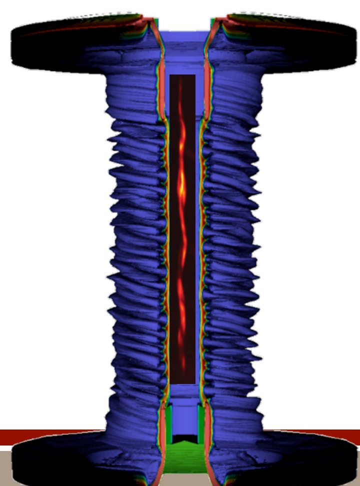

Resulting weakly helical (dr << dz) emitting stagnation column remains quasi-2D such that $P_{stag}^{exp} \sim P_{stag}^{3D} \sim P_{stag}^{2D} \sim 1$ Gbar

Analysis suggests the MagLIF platform is stable to high convergence, produces the expected P_{stag}, and is not dominated by 3D physics in the hot spot.

Experimental neutron spectra from z2591

primary

$$D + D \underset{50\%}{\rightarrow} He^3 \ (0.82\, MeV) + n \ (2.45\, MeV)$$

$$D + D \underset{50\%}{\rightarrow} T \ (1.01\, MeV) + p \ (3.02\, MeV)$$

secondary

$$D + T \rightarrow He^4 \ (3.52\, MeV) + n \ (14.1\, MeV)$$

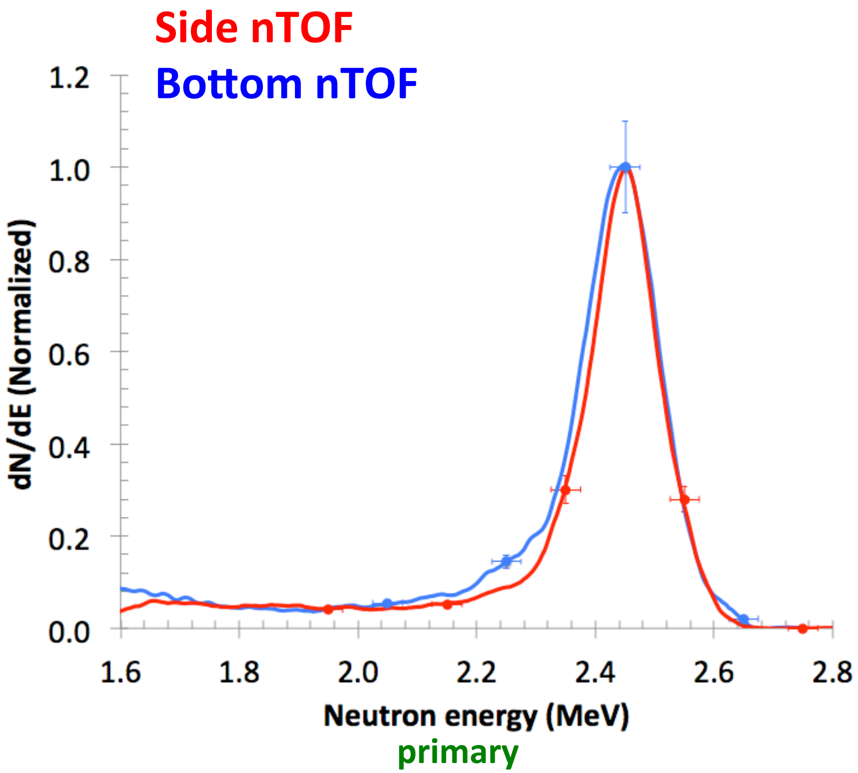

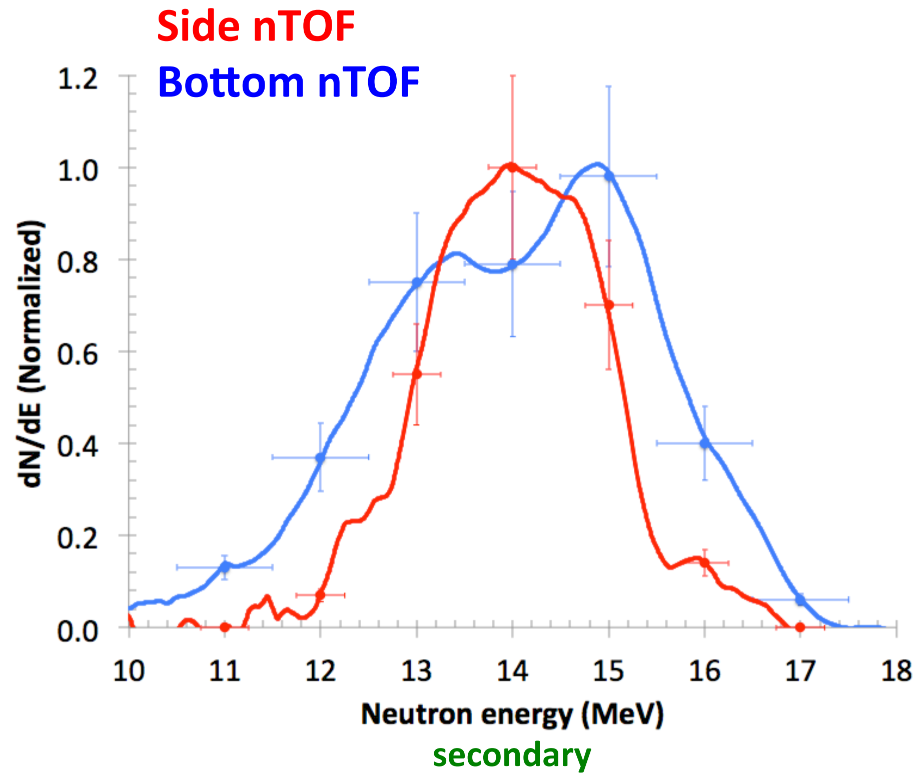

SAND2015-5089 C

Particle (PIC) simulations are used to generate synthetic neutron spectra

LSP simulations are initialized with HYDRA output (n, T, B) just before stagnation, and then run through burn.

All ions are evolved kinetically

$$D + D \underset{50\%}{\rightarrow} He^3 \ (0.82\,MeV) + n \ (2.45\,MeV)$$

$$D + D \underset{50\%}{\rightarrow} T \ (1.01\,MeV) + p \ (3.02\,MeV)$$

$$D + T \rightarrow He^4 \ (3.52\,MeV) + n \ (14.1\,MeV)$$

Synthetic neutron detectors are located to the side, top, and bottom of the stagnation column

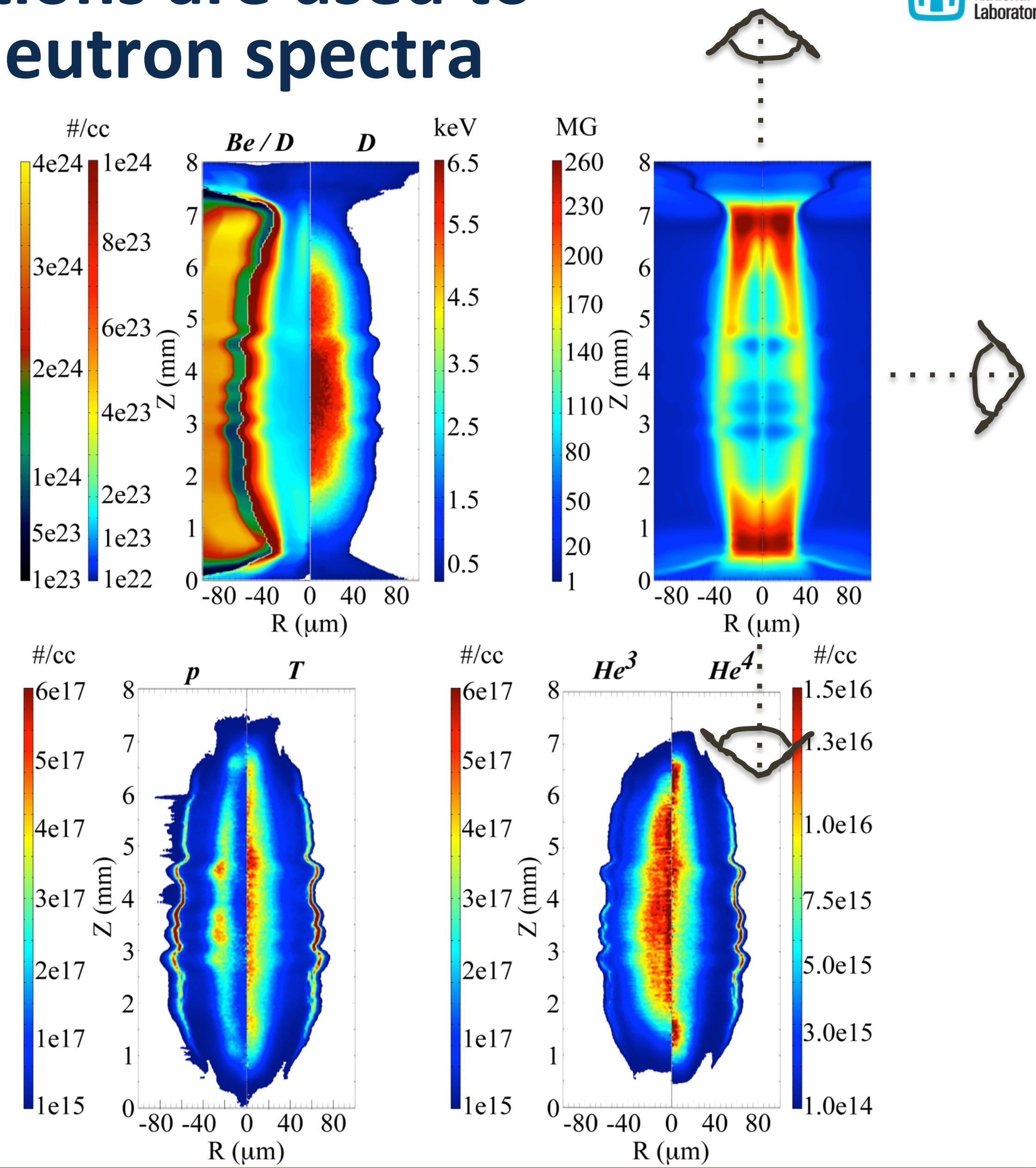

Comparison of neutron spectra

$$D + D \underset{50\%}{\rightarrow} He^3 \ (0.82\ MeV) + n\ (2.45\ MeV)$$ (primary)

$$D + D \underset{50\%}{\rightarrow} T\ (1.01\ MeV) + p\ (3.02\ MeV)$$

$$D + T \rightarrow He^4\ (3.52\ MeV) + n\ (14.1\ MeV)$$ (secondary)

primary

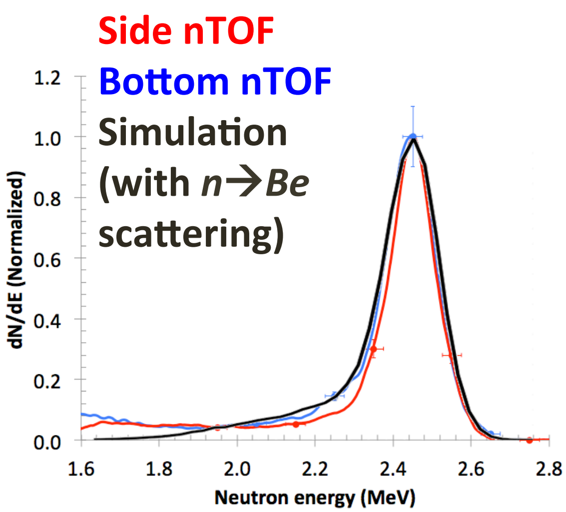

secondary

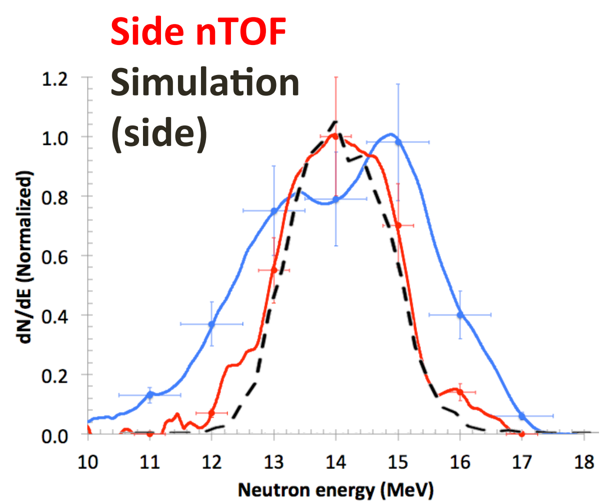

secondary

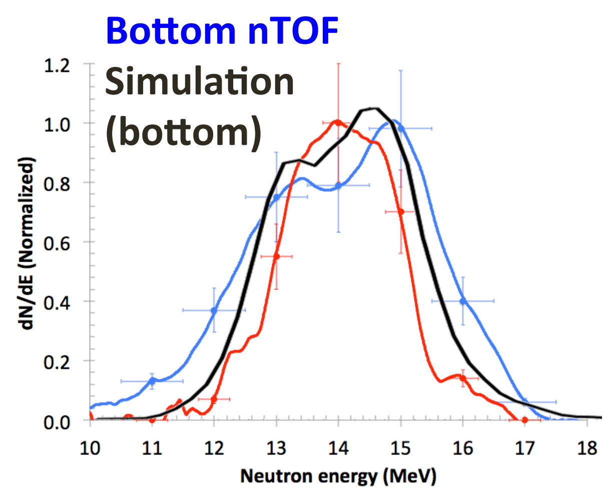

Simulation

$Y_n^{DD} = 2.5e12$

$Y_n^{DD}/Y_n^{DT} = 49$

Experiment

$Y_n^{DD} = (2.0 \pm 0.5)e12$

$Y_n^{DD}/Y_n^{DT} = 40 \pm 20$

Comparison of liner emission

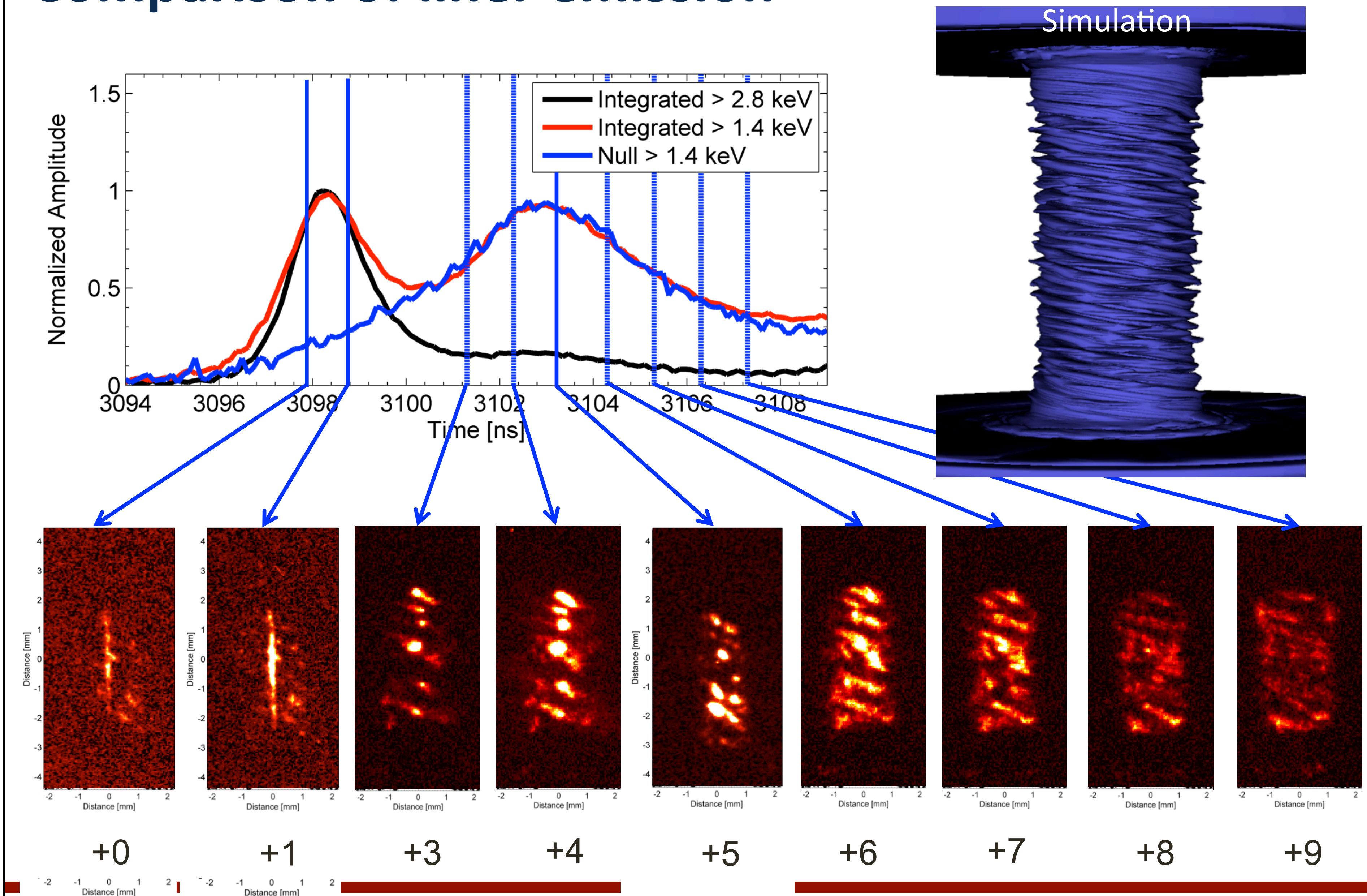

Comparison of liner emission

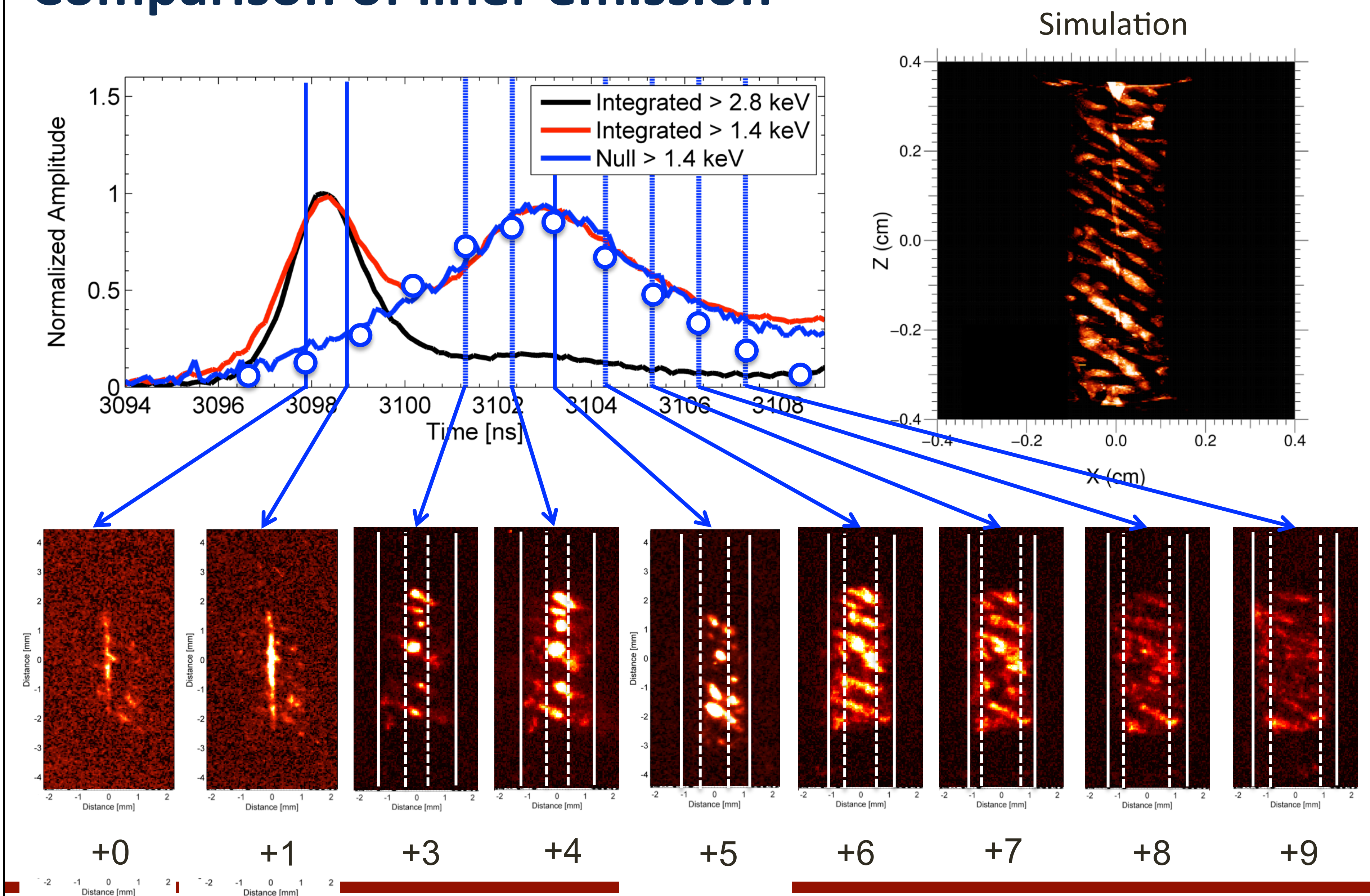

Comparison between observables and post-shot degraded 2D & 3D simulations

Sandia National Laboratories

Parameter	Measured/inferred [z2591]	Post-shot simulations
I_{max}	19 ± 1.5 MA	19 MA
t_{imp}^{5MA}	+90 ± 1 ns	+90 ns (~70 km/s)
r_{laser}	450 ± 150 μm	450 ± 150 μm
E_{gas}^{abs}	~100-300 J	200 ± 50 J
r_{stag}^{hot}	44 ± 13 μm	40 μm (r_{stag}^{liner} 53 μm, CR_{2D}^{liner} 44)
$\langle T_i \rangle^{DD}$, $\langle T_{i,e}^{spec} \rangle$	2.5 ± 0.75, 3.0 ± 0.5 keV	3.0 ± 0.5, 2.7 ± 0.5 keV
ρ_{gas}^{stag}, m_{loss}	0.3 ± 0.2 g cm^{-3}, ~70%	0.4 ± 0.2 g cm^{-3}, 61%
ρR_{gas}, ρR_{liner}^{stag}	2 ± 1, 900 ± 300 mg cm^{-2}	2.6 ± 1.0, 900 mg cm^{-2}
$\langle P^{stag} \rangle$, E_{gas}^{stag}	1.0 ± 0.5 Gbar, 4 ± 2 kJ	1.5 ± 0.3 Gbar, 7 ± 2 kJ
$\langle B_z^f r_{stag} \rangle$	(4.5±0.5)e5 G cm ($r_{stag}/r_{L,\alpha}$ 1.7)	4.8e5 G cm ($r_{stag}/r_{L,\alpha}$ 1.8) ($\langle B_z^f \rangle$ 91 MG)
Y_n^{DD}	(2.0±0.5)e12	(2.5±0.5)e12
Y_n^{DD}/Y_n^{DT}	40 ± 20	41-57
DD, DT spectra	isotropic, asymmetric	isotropic, asymmetric
t_{burn}^{FWHM}	2.3 ± 0.6 ns (x-rays) [z2591, Y_n^{DD}=2e12] 1.5 ± 0.1 ns (x-rays) [z2613, Y_n^{DD}=1e12]	1.6 ± 0.2 ns (neutrons and x-rays)
Liner emission	bounce & peak emission: t_{stag}+5 ns	bounce & peak emission: t_{stag} +5 ns
Δz_{burn} shape	6 mm, helical	6 mm, helical
mix	10 ± 10 %, not ≥ 20%	0% (by design), {Recent expts: ~ < 5%}

Without phase plates or beam smoothing, unstable laser-plasma interaction expected!

OMEGA-EP
750um DPP

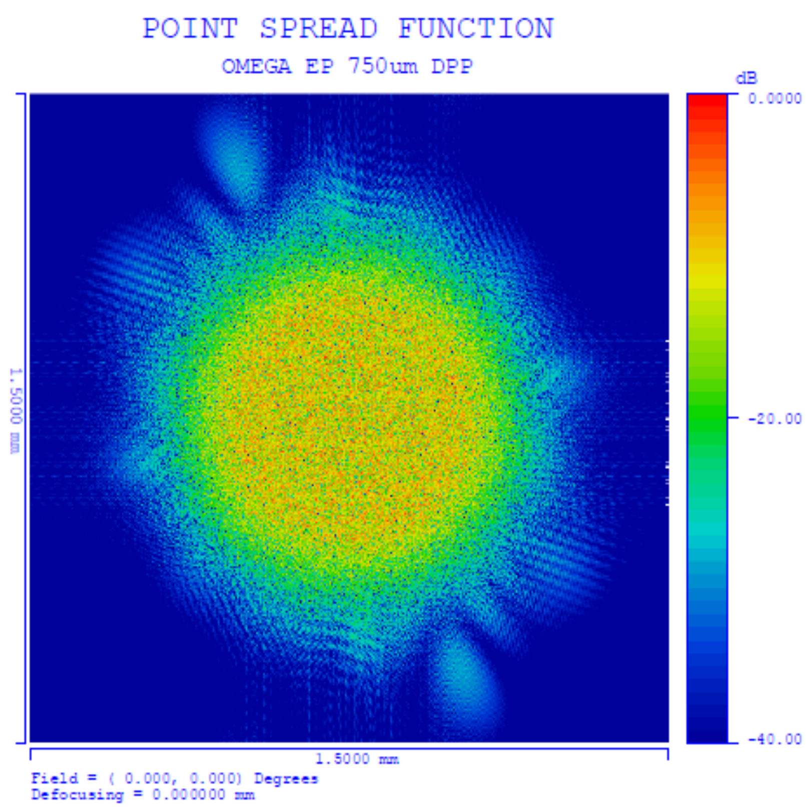

ZBL (Z-Beamlet [NIF prototype])
No DPP (representative)

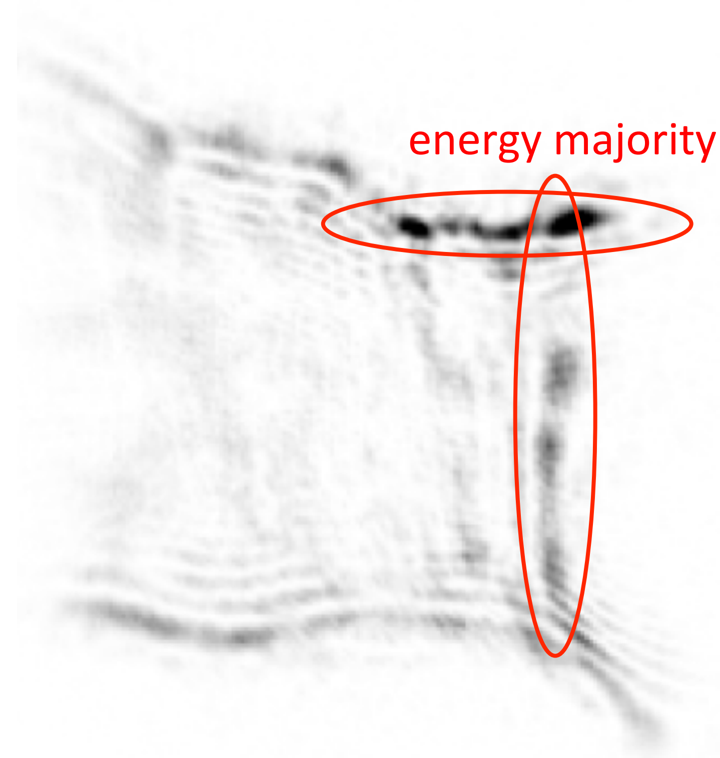

In the beginning, we had to make progress without this critical technology

Laser-only experiment:
Blastwave measurements via VISAR

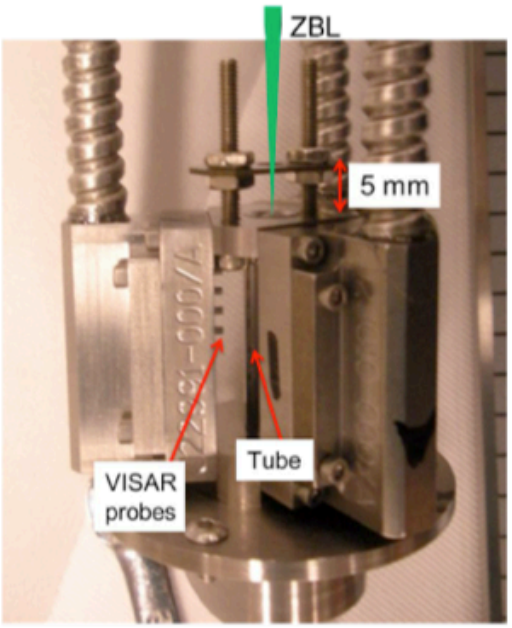

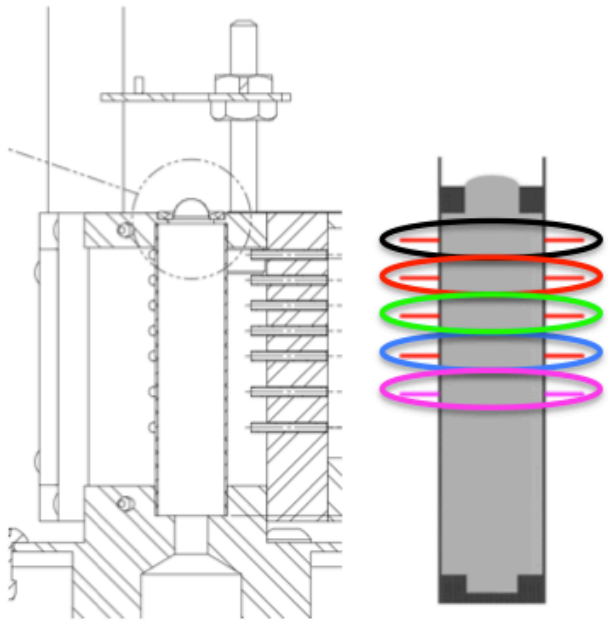

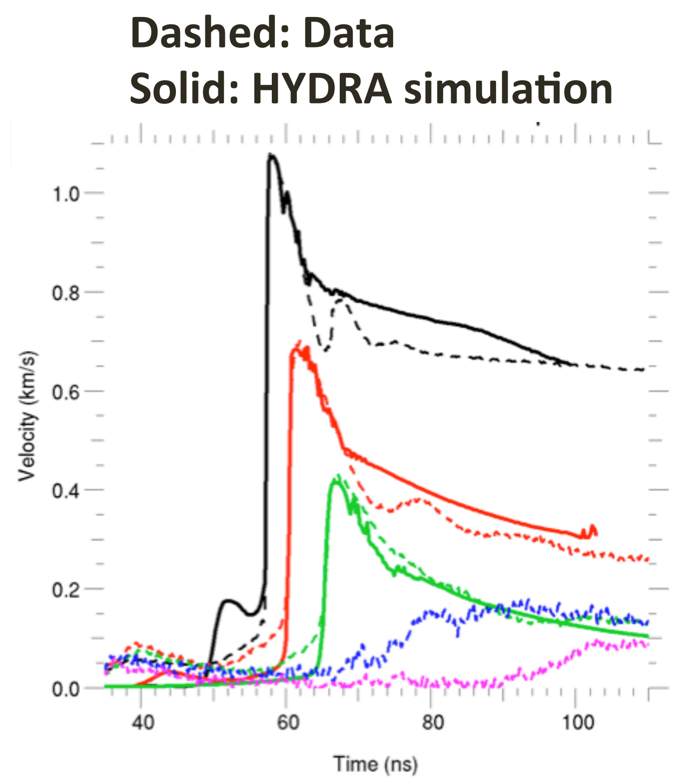

Inferred: 330 J or less coupled to the gas (of ~2.8 kJ)

Laser-only experiment:
Shots in Z chamber with x-ray diagnostics

Two separate diagnostics confirmed heating:

Inferred peak <T_e>~500 eV (equilibration value lower)

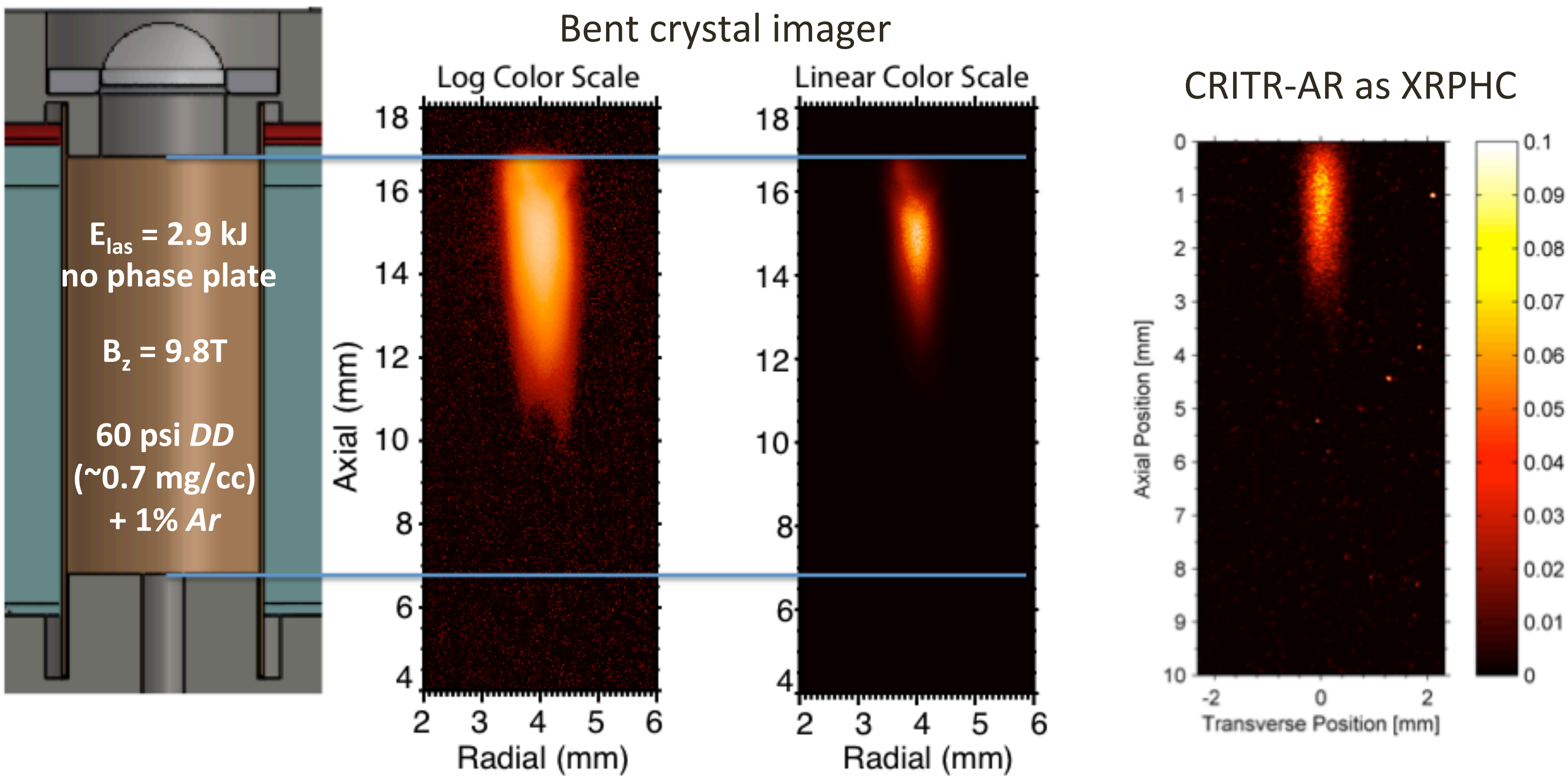

Radial and axial extents of heated plasma region match up on both linear and log scales

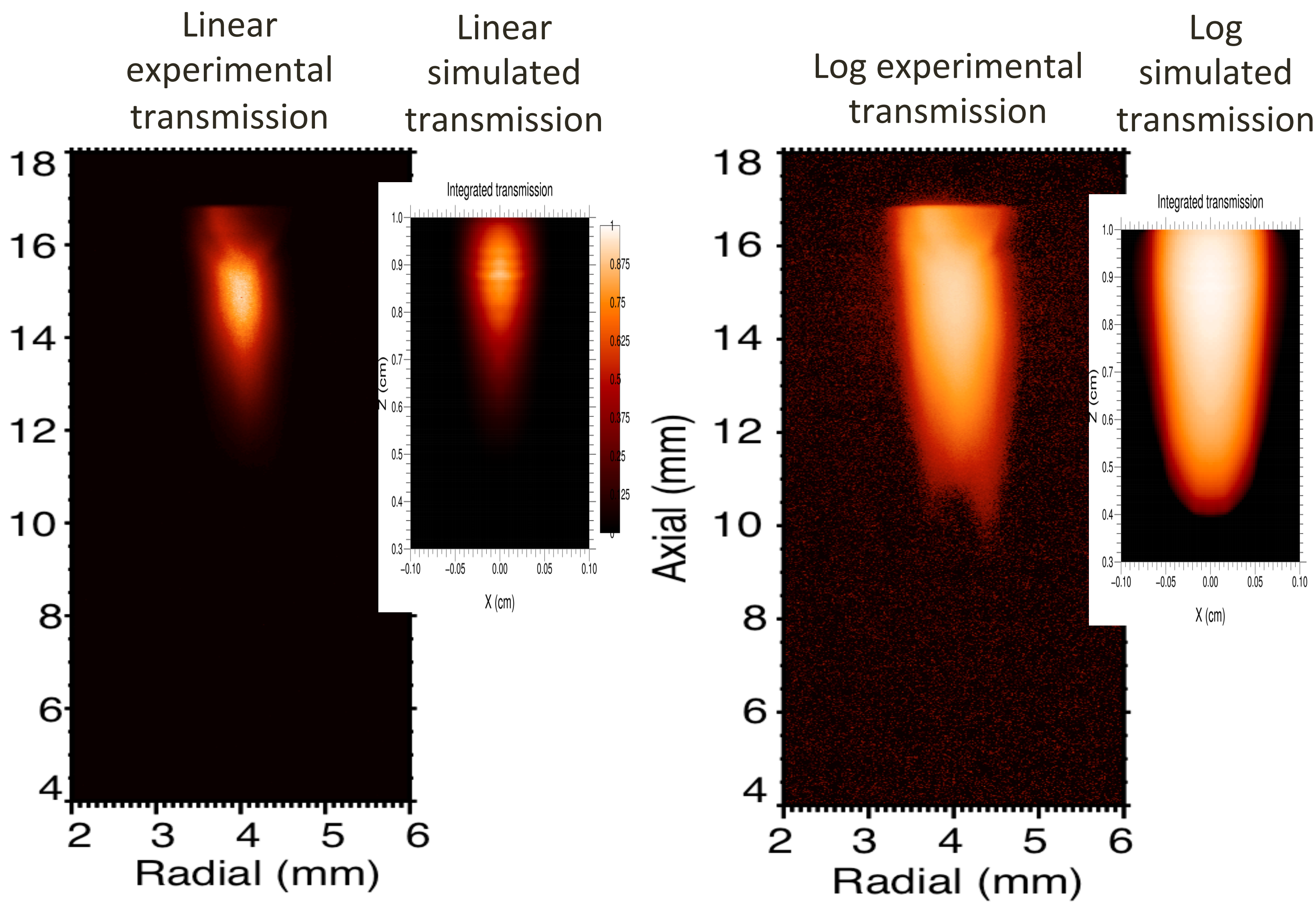

Normalized x-ray images from two diagnostics compare favorably to calculated distribution

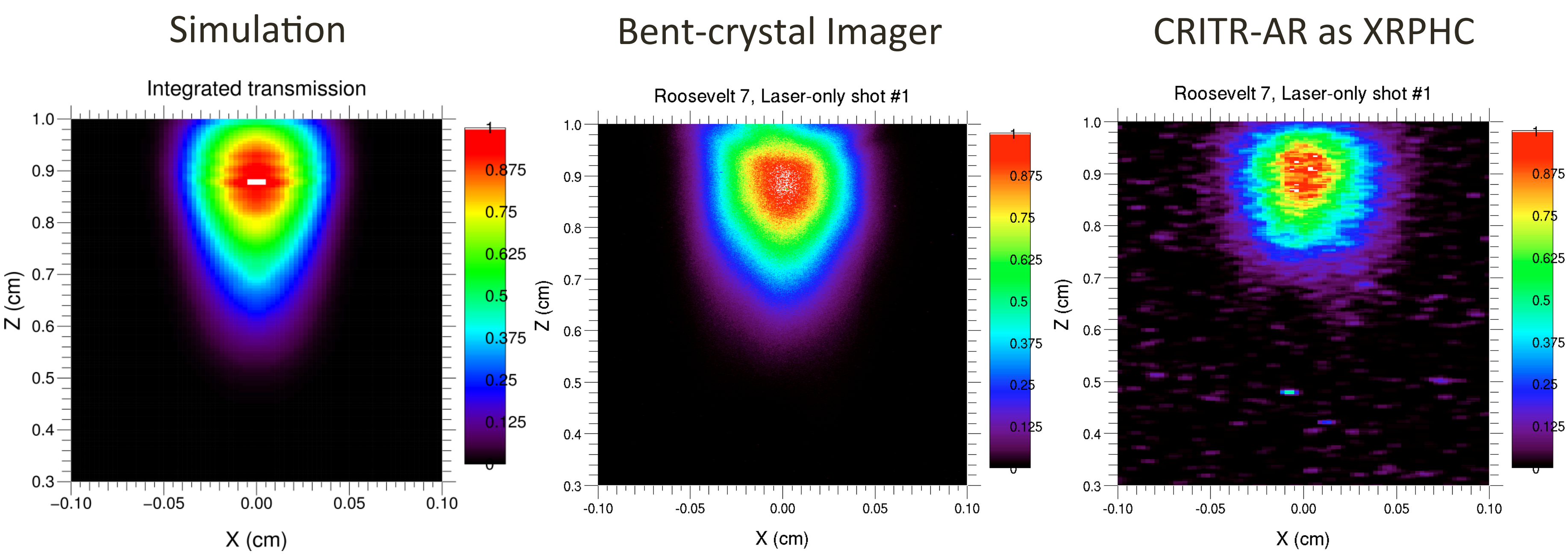

Inferred: Only ~200 J coupled through 1.5 μm foils (of ~2-3 kJ)

Simulations suggest the LEH channel is a source of undesirable levels of non-fuel mix

In high-resolution calculations, **mix threats from the window and LEH** are present due to radiation ablation and shockwaves, and high-Z materials can move into the gas quickly.

dr ~ 350 μm of inner LEH material ablated, interacts with blastwave

window material jets forward into gas

dr ~ 100 μm of inner liner wall ablated

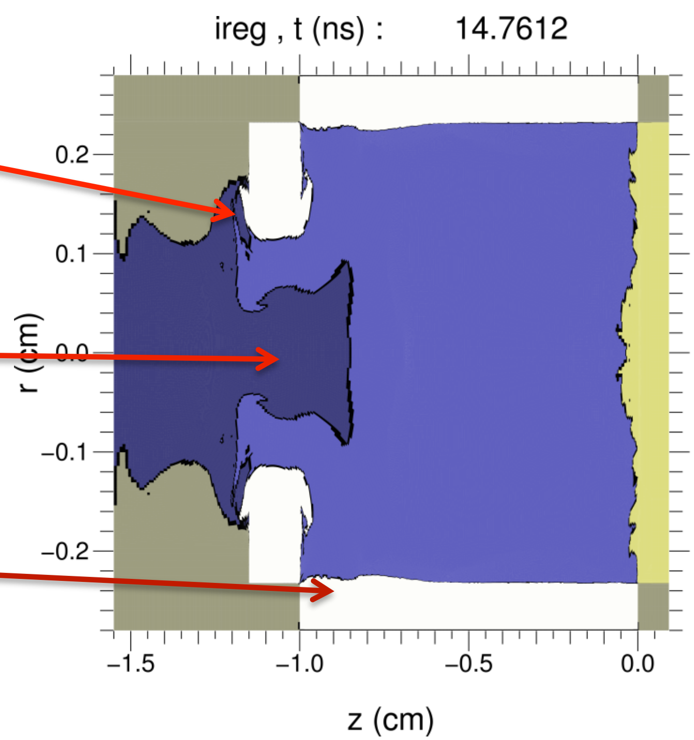

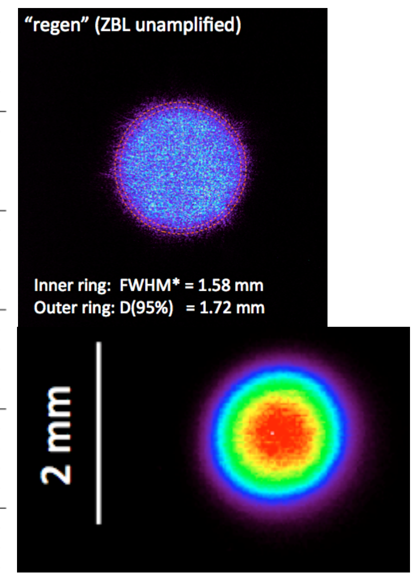

In the absence of significant mix, simulations suggest > 10^{13} yields are possible on Z

Simulations:
Increasing laser energy (E_{laser}) from 200 J absorbed to > 1 kJ should *dramatically increase* yield (in absence of mix)

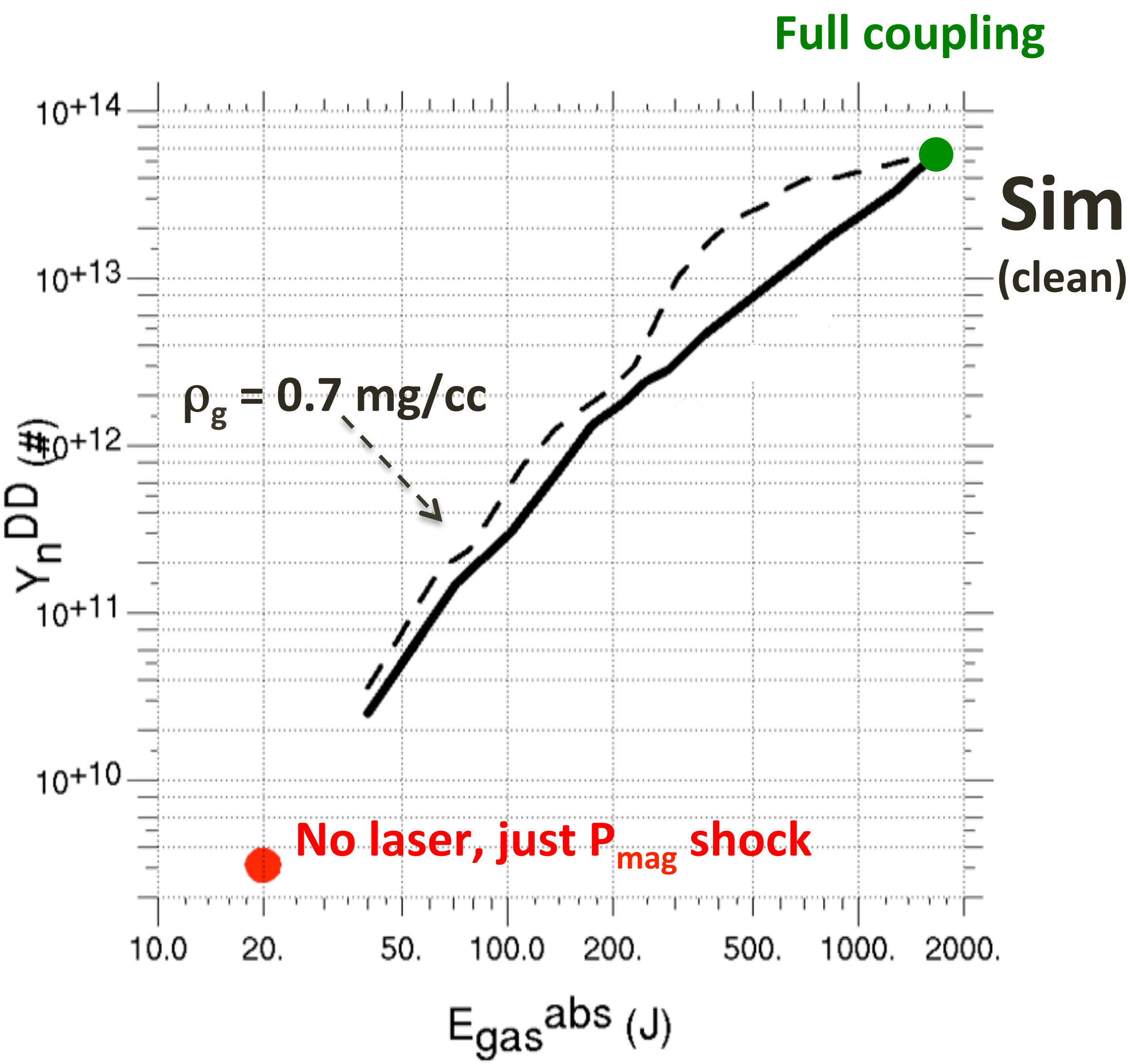

To date, increased laser energy has reduced yield, consistent with *Z**>1 mix from the window and LEH

Simulations:
Increasing laser energy (E_{laser}) from 200 J absorbed to > 1 kJ should *dramatically increase* yield (in absence of mix)

Experiments to-date:
Target changes thought to *increase* laser absorption into gas have all *decreased* the yield.

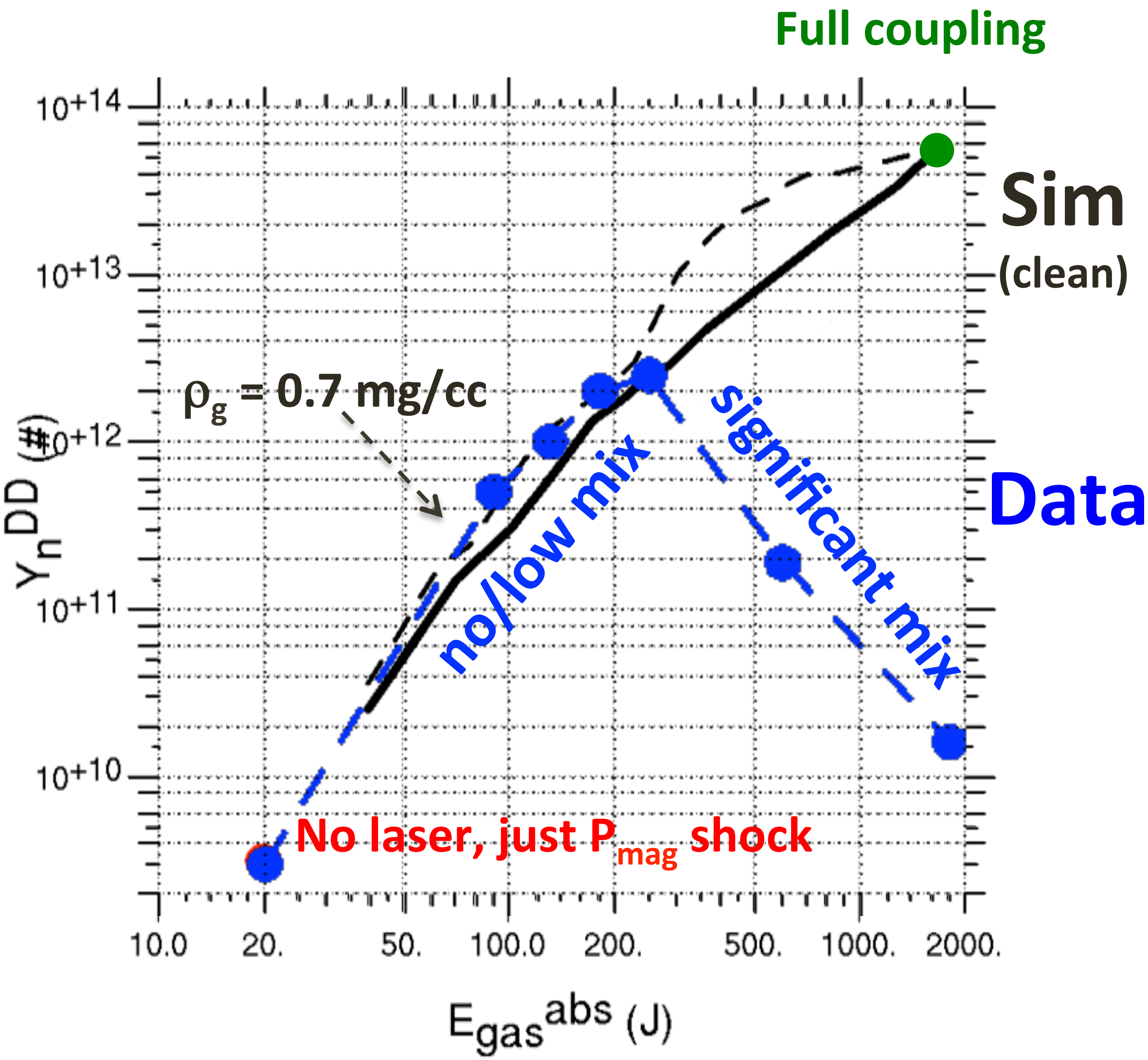

To date, increased laser energy has reduced yield, consistent with *Z**>1 mix from the window and LEH

Simulations:
Increasing laser energy (E_{laser}) from 200 J absorbed to > 1 kJ should *dramatically increase* yield (in absence of mix)

Experiments to-date:
Target changes thought to *increase* laser absorption into gas have all *decreased* the yield.

Laser-produced mix (direct or indirect via blastwave or radiation) appears to be the culprit.

Must stay unmixed for ~60 ns!

We can dud the top of the stagnation plasma!

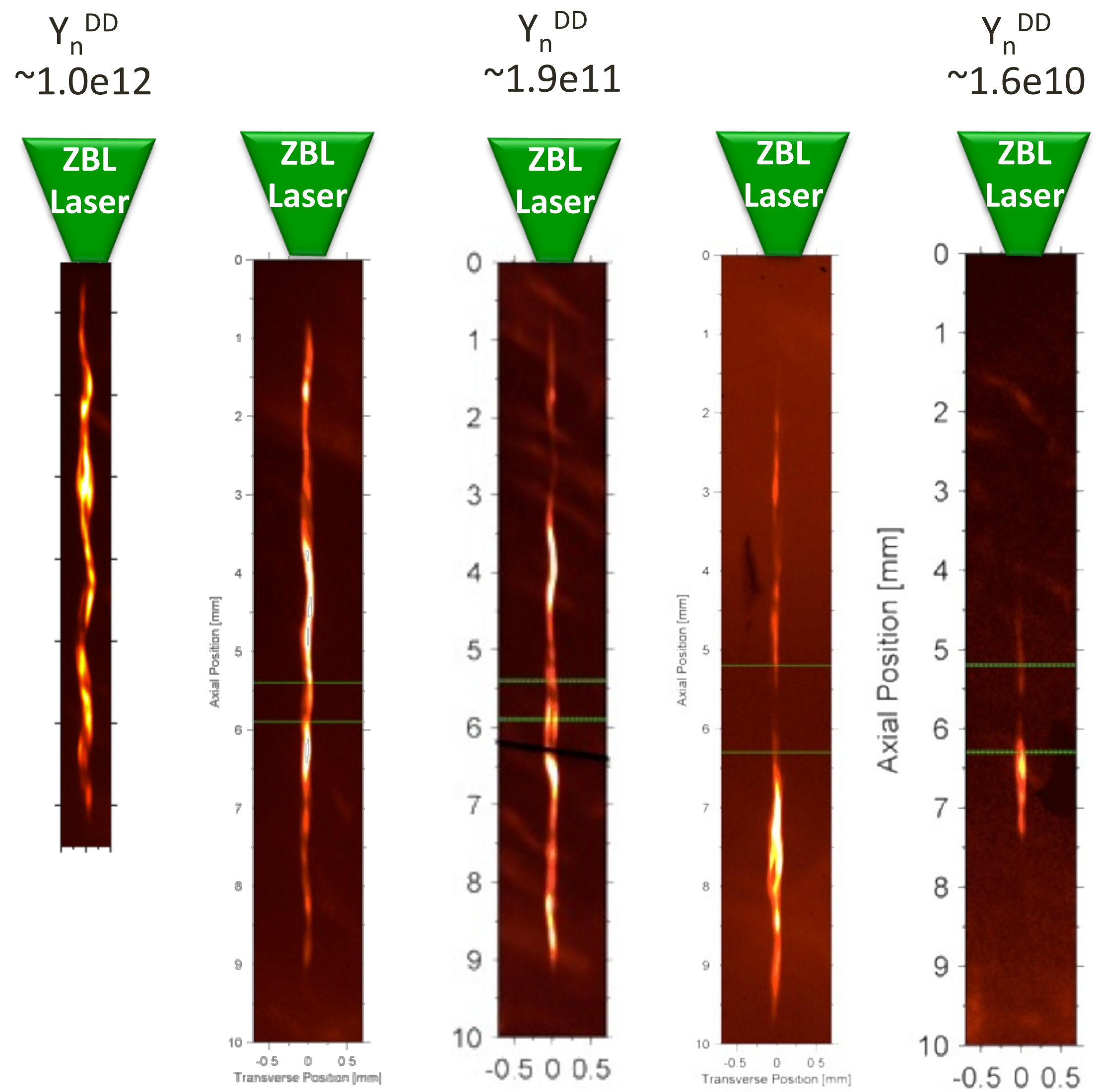

Upcoming experiments will test a redesigned target meant to reduce laser-produced mix

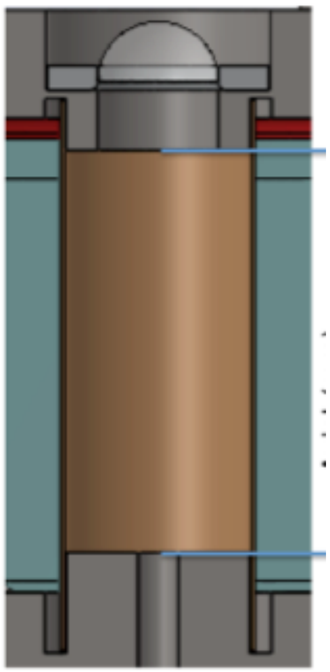

Old target:	New target (cryo):
1.5 mm standoff between window and imploding region	5.0 mm standoff (window has to move farther to mix)
1.5-3.5 micron window thicknesses	0.25-0.4 micron (3-9x mass reduction)
3 mm ID LEH	4.6 mm ID LEH
CH and/or *Al* components in LEH and beam dump	None (laser only sees *Be*)
Either no phase plate or 1.8 mm phase plate	0.7 mm phase plate

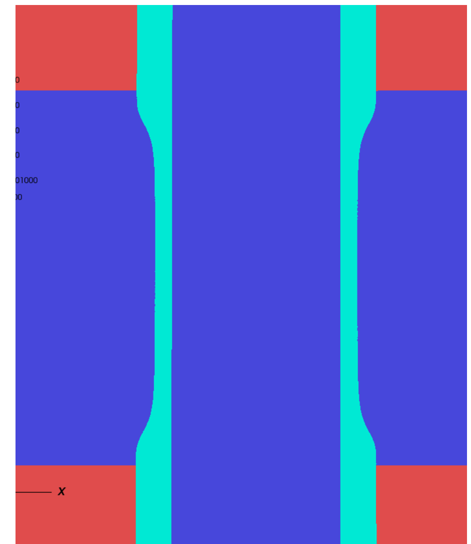

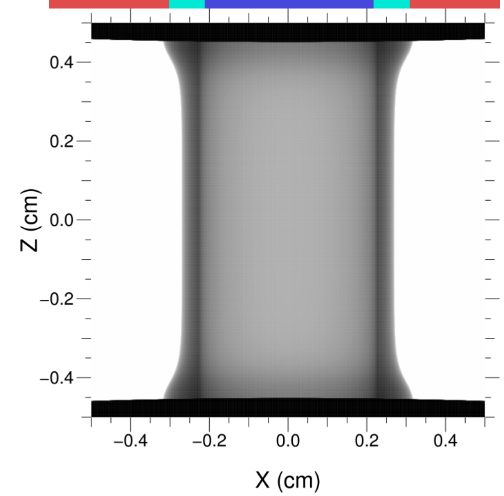

Summary

We seek to understand and improve the MagLIF platform, and demonstrate expected yield scaling (laser energy, B_z field, current, etc.)

MagLIF enables ICF yields at Z using slow and stable implosions, with large >40 convergence ratios

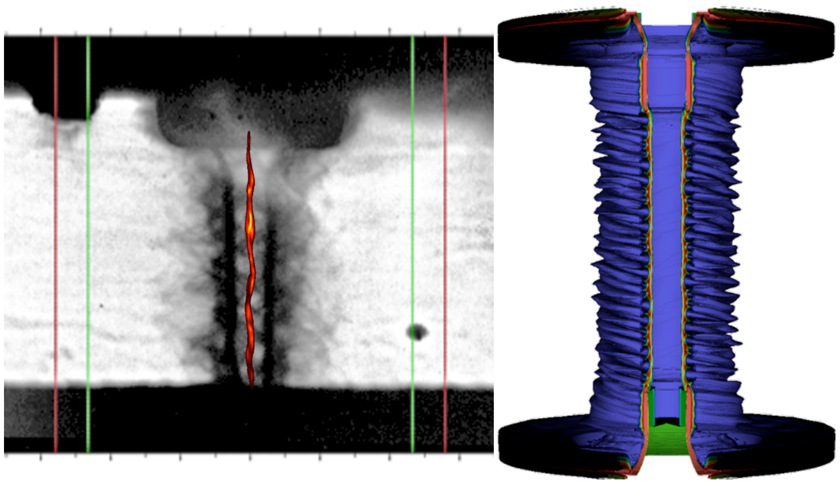

Magnetized laser-preheating focused experiments help us understand heating and mix

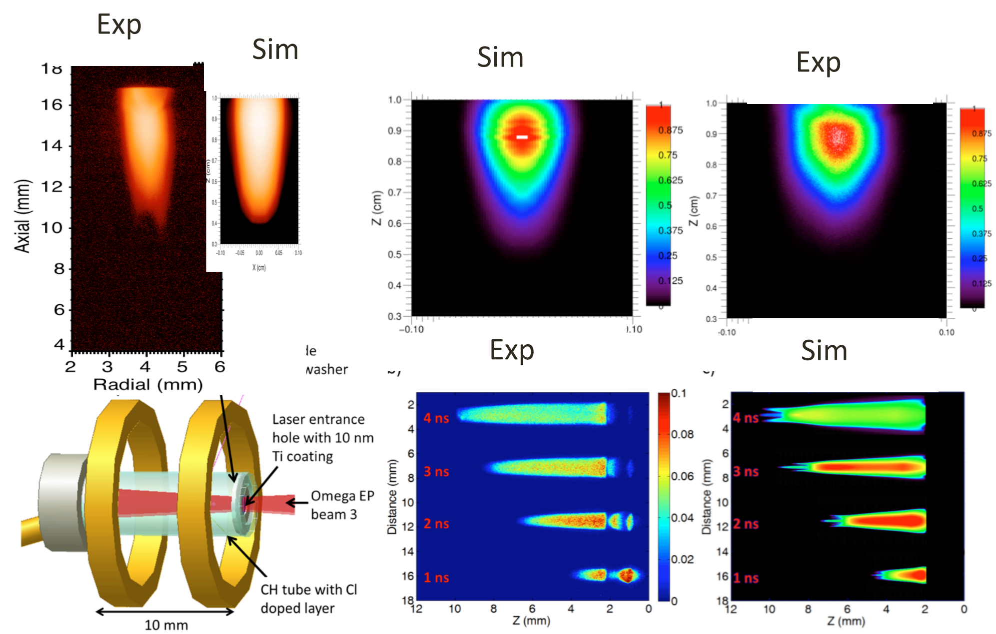

Figure 1: a) Proposed target design; b) experimental framing camera images showing the propagation of a 4 ns long, 3 kJ OMEGA EP beam through a pure Ar gas at several times; c) Simulated images of the experiment from HYDRA.

See talk by A. J. Harvey-Thompson at this conference